

The Relativistic Bound State Problem in QCD: Transverse Lattice Methods

Matthias Burkardt
Department of Physics,
New Mexico State University , Las Cruces, NM 88003, U.S.A.

Simon Dalley
Centre for Mathematical Sciences,
Cambridge University, Wilberforce Road Cambridge CB3 0WA, England

October 30, 2018

Abstract

The formalism for describing hadrons using a light-cone Hamiltonian of $SU(N)$ gauge theory on a coarse transverse lattice is reviewed. Physical gauge degrees of freedom are represented by disordered flux fields on the links of the lattice. A renormalised light-cone Hamiltonian is obtained by making a colour-dielectric expansion for the link-field interactions. Parameters in the Hamiltonian are renormalised non-perturbatively by seeking regions in parameter space with enhanced Lorentz symmetry. In the case of pure gauge theories to lowest non-trivial order of the colour-dielectric expansion, this is sufficient to determine accurately all parameters in the large- N limit. We summarize results from applications to glueballs. After quarks are added, the Hamiltonian and Hilbert space are expanded in both dynamical fermion and link fields. Lorentz and chiral symmetry are not sufficient to accurately determine all parameters to lowest non-trivial order of these expansions. However, Lorentz symmetry and one phenomenological input, a chiral symmetry breaking scale, are enough to fix all parameters unambiguously. Applications to light-light and heavy-light mesons are described.

Contents

1	Introduction	2
1.1	<i>Boundstates in light-cone co-ordinates</i>	3
1.2	<i>Physical motivation for light-cone framework</i>	6
2	Pure transverse lattice gauge theory	10
2.1	<i>Colour-dielectric formulation of the light-cone Hamiltonian</i>	10
2.2	<i>Determination of Fock space eigenfunctions</i>	14

2.3	<i>Confinement of heavy sources</i>	19
2.4	<i>Simplification in the Large N limit</i>	22
3	A solution of pure gauge theory at large N	24
3.1	<i>Topography of coupling space</i>	26
3.2	<i>Results for glueball boundstates</i>	28
4	Mesons on the transverse lattice	30
4.1	<i>Formulation of the light-cone Hamiltonian with fermions</i>	30
4.2	<i>Numerical studies of light mesons</i>	34
4.3	<i>B mesons on the transverse lattice</i>	43
5	Summary and Outlook	46
A	Miscellaneous Remarks about Fermions	48
A.1	<i>Momentum dependent mass counterterms</i>	49
A.2	<i>Vertex mass renormalisation</i>	50
A.2.1	<i>Three point vertex in the chiral limit</i>	50
A.2.2	<i>Fock sector dependent vertex renormalisation</i>	51

1 Introduction

Relativistic strongly-bound states in generic four-dimensional gauge theories represent a formidable theoretical challenge. Future progress in particle physics is likely to hinge upon a detailed theoretical understanding of these questions, since they are both of intrinsic interest in hadronic and nuclear physics, and important for the proper identification of new physics beyond the Standard Model. This has led to the development of Hamiltonian quantisation on a light-front. In the presence of suitable high-energy cut-offs, the light-cone vacuum state is trivial and constituent-like wavefunctions can be built upon it in a Lorentz boost-invariant fashion. In fact, these light-cone wavefunctions carry all the non-perturbative, coherent information about bound and scattering states in a general Lorentz frame. This review is about a particular non-perturbative method of formulating and solving the light-cone Hamiltonian problem of non-abelian gauge theories — the transverse lattice method [1] — with emphasis on QCD and hadronic structure. It is particularly well suited to the scale of the strong interactions between short distances described by asymptotically free QCD and the relatively long range phenomena of nuclear forces. A successful description of this intermediate region should not only include ‘global’ properties of hadrons, such as masses and decay constants, but also the wealth of experimental data on hadronic sub-structure, such as structure functions, form factors, and distribution amplitudes. All of these observables are simply related to light-cone wavefunctions.

The transverse lattice method brings together two powerful ideas in quantum field theory: light-cone Hamiltonian quantisation and lattice gauge theory. For readers unfamiliar with the light-cone framework, we provide a brief introduction to its salient points in the rest of this chapter. There exist a number of recent and more extensive reviews on the theory and applications of light-cone quantisation [2, 3]. For this reason we omit any detailed description of light-cone approaches other than the transverse

lattice in this article. No special knowledge of lattice gauge theory is needed for this review, although an understanding at the level of introductory chapters of textbooks [4] would no doubt be useful.

An important ingredient in the formulation of transverse lattice gauge theory we expound here, is the colour-dielectric expansion. We characterise a dielectric formulation as one in which physical gluon fields, or rather the $SU(N)$ group elements they generate, are replaced by collective variables which represent an average over the fluctuations on short distance scales. These dielectric variables carry colour and form an effective gauge field theory with classical action minimised at zero field, meaning that colour flux is expelled from the vacuum at the classical level. The price one pays for starting with a simple vacuum structure, which arises only for a rather low momentum cut-off on the effective theory, is that the effective cut-off Hamiltonian is initially poorly constrained. We will demonstrate, however, that the colour-dielectric expansion, together with requirements of symmetry restoration, is sufficient to organise the interactions in the Hamiltonian in a way suitable for practical solution. To date, all such solutions have been obtained in the limit of large number of colours $N \rightarrow \infty$ of $SU(N)$ gauge theories. For this reason, the kinds of bound state that have been investigated have been limited to glueballs and mesons. Although the $N \rightarrow \infty$ limit simplifies calculations, it is not necessary, and in principle baryons can also be treated in the same framework.

A number of more well-established techniques exist for studying boundstate problems of quarks and gluons in non-abelian gauge theory, not to mention the many possible approaches that treat some or all of the boundstates as effective degrees of freedom in themselves. Typically, there is a (computational) trade-off between the output detail that one can predict and the amount of information one must input from experiment; one is always hoping for a high output/input ratio. Lattice gauge theory, of which there are many variants, treats the problems from first principles. This means that symmetry alone determines the output of the calculation and no data are taken from experiment, aside from parameters that are undetermined in QCD (such as the confinement scale or quark masses). However, the number of things one can reasonably compute in practice is much less than one would like. One advantage of a lattice method that computes light-cone wavefunctions, such as the transverse lattice gauge theory, is that a single calculation leads to estimates of a wide range of observables.

Boundstate calculations are made easier if one is prepared to take some discrete information from experiment, such as values of condensates as used in QCD sum rules [5]. Still greater predictive power is obtained if aspects of the gauge theory are modelled, for example by using models of the vacuum [6] to determine condensates used in sum rules, or models of vertex functions and propagators to be used in truncations of Dyson-Schwinger equations [7]. We will suggest that the colour-dielectric formulation of transverse lattice gauge theory can, with reasonable effort, yield fairly accurate output from first principles, or at worst from a small amount of discrete experimental input. On the other hand, it contains within its solutions the entire amplitude structure of hadrons at resolutions of order 1/2 fermi and above; it has a high output/input ratio.

1.1 *Boundstates in light-cone co-ordinates*

We denote the co-ordinate four vector $(t, \vec{x}) = (x^0, (x^1, x^2, x^3))$. In light cone co-ordinates $x^\pm = x_\mp = (x^0 \pm x^3)/\sqrt{2}$, $\mathbf{x} = (x^1, x^2)$, and x^+ is treated as the canonical ‘time’ variable, i.e. the (light-cone) wavefunction is defined on a null-plane $x^+ = \text{constant}$. The Lorentz indices $\mu, \nu \in \{0, 1, 2, 3\}$ are split into light-cone indices $\alpha, \beta \in \{+, -\}$ and transverse indices $r, s \in \{1, 2\}$ (we automatically sum over repeated raised and lowered indices). Since x^3 is an arbitrarily chosen space direction, this formulation

lacks manifest rotational invariance. However, the null-plane possesses manifest boost invariance, this being ultimately more useful for relativistic problems. One might imagine that the light-cone framework therefore bears no relation to nonrelativistic quantum mechanics (NRQM). However, there is an isomorphism between the structure of many-particle states in both cases [8], which is the first hint of the utility of light-cone co-ordinates in the description of relativistic boundstates.

Boost (Galilei) transformations in NRQM

$$\vec{x}' = \vec{x} + \vec{v}t \quad (1)$$

$$t' = t \quad (2)$$

are purely kinematic because they leave the quantization surface $t = 0$ invariant. This property has important consequences for a many body system. For example, wavefunctions in the rest frame and in a boosted frame are related by a simple shift of (momentum) variables \vec{p} , e.g. for a two-body system boosted by velocity \vec{v} the wavefunction behaves as

$$\psi_{\vec{v}}(\vec{p}_1, \vec{p}_2) = \psi_{\vec{0}}(\vec{p}_1 - m_1\vec{v}, \vec{p}_2 - m_2\vec{v}). \quad (3)$$

Furthermore, if the Hamiltonian is translationally invariant, the dynamics of the *center of mass*

$$\vec{R} = \sum_i x_i \vec{r}_i, \quad (4)$$

with $x_i = m_i/M$ the mass fraction of particle i and $M = \sum_i m_i$, separates from the intrinsic variables, making it possible to work in the center of mass frame.

One of the features that normally complicates the description of relativistic bound states is that equal t hyperplanes are not invariant under relativistic boosts

$$\mathbf{x}' = \mathbf{x} \quad (5)$$

$$x^{3'} = \gamma (x^3 + vx^0) \quad (6)$$

$$x^{0'} = \gamma \left(x^0 + \frac{v}{c^2} x^3 \right), \quad (7)$$

with $\gamma^{-2} = 1 - \frac{v^2}{c^2}$. As a result, boosts are in general a dynamical operation; the generator of boost transformations contains interactions and there exists no simple generalization of Eq. (3) to a relativistic system quantized at equal x^0 . Furthermore, the notion of the center of mass has no useful generalization in such an equal- x^0 quantized relativistic framework.

One of the advantages of the light-cone framework, where quantisation is performed at equal- x^+ null-planes, is that there is a subgroup of kinematical boosts among the generators of the Poincaré group [9]. To see this let us start from the usual Poincaré algebra

$$[P^\mu, P^\nu] = 0 \quad (8)$$

$$[M^{\mu\nu}, P^\rho] = i(g^{\nu\rho}P^\mu - g^{\mu\rho}P^\nu) \quad (9)$$

$$[M^{\mu\nu}, M^{\rho\lambda}] = i(g^{\mu\lambda}M^{\nu\rho} + g^{\nu\rho}M^{\mu\lambda} - g^{\mu\rho}M^{\nu\lambda} - g^{\nu\lambda}M^{\mu\rho}) \quad (10)$$

where the generators of rotations and boosts are respectively $J_i = \frac{1}{2}\varepsilon_{ijk}M_{jk}$ and $K_i = M_{i0}$. We now introduce transverse boost-rotation operators

$$B_1 = \frac{1}{\sqrt{2}}(K_1 + J_2) \quad (11)$$

$$B_2 = \frac{1}{\sqrt{2}}(K_2 - J_1) \quad (12)$$

so $B_r = -M_{-r}$. It follows from the Poincaré algebra that these satisfy commutation relations

$$[J_3, B_r] = i\varepsilon_{rs}B_s \quad (13)$$

$$[P_r, B_s] = -i\delta_{rs}P^+ \quad (14)$$

$$[P^-, B_r] = -iP_r \quad (15)$$

$$[P^+, B_r] = 0 \quad (16)$$

where $\varepsilon_{12} = -\varepsilon_{21} = 1$, and $\varepsilon_{11} = \varepsilon_{22} = 0$. Together with the well known commutation relations

$$[J_3, P_r] = i\varepsilon_{rs}P_s \quad (17)$$

$$[P^-, P_r] = [P^-, P^+] = [P^-, J_3] = 0 \quad (18)$$

$$[P^+, P_r] = [P^+, B_r] = [P^+, J_3] = 0 \quad (19)$$

these are the same relations as the commutators among the generators of the Galilei transformations for NRQM in the plane, provided we make the identifications

$$P^- \longrightarrow \text{Hamiltonian} \quad (20)$$

$$\mathbf{P} = (P^1, P^2) \longrightarrow \text{momentum in the plane} \quad (21)$$

$$P^+ \longrightarrow \text{mass} \quad (22)$$

$$J_3 \longrightarrow \text{rotations around } x^3\text{-axis} \quad (23)$$

$$\mathbf{B} = (B^1, B^2) \longrightarrow \text{generator of boosts in the plane,} \quad (24)$$

i.e. $e^{i\mathbf{v}\cdot\mathbf{B}}\mathbf{P}e^{-i\mathbf{v}\cdot\mathbf{B}} = \mathbf{P} + P^+\mathbf{v}$. Because of this isomorphism between transverse boost-rotations in light-cone coordinates and boosts in the context of NRQM in the plane, many familiar results from NRQM can be directly carried over to relativistic systems. In particular, since the longitudinal momentum fractions $x_i \equiv k_i^+/P_{total}^+$ play a role very similar to the mass fractions m_i/M_{total} in NRQM, it is very natural that we find as a reference point for distributions in the transverse plane the *transverse center of momentum*

$$\mathbf{R} = \frac{\sum_i k_i^+ \mathbf{r}_i}{P_{total}^+} = \sum_i x_i \mathbf{r}_i, \quad (25)$$

where k_i^+ and \mathbf{r}_i are the longitudinal momentum and transverse position of the i^{th} particle respectively. Moreover, the fractions x_i , like masses in NRQM, are invariant under all the boosts K_i (K_3 rescales longitudinal momentum).

The Hamiltonian, which evolves the light-cone wavefunction in light-cone time x^+ , is $P^- = (P^0 - P^3)/\sqrt{2}$, where P^0 is the usual energy. Both P^- and the light-cone momentum $P^+ = (P^0 + P^3)/\sqrt{2}$

are positive definite for massive particles. This simple observation has the important consequence that the vacuum state, which has $P^+ = 0$, cannot mix with massive particle (parton) degrees of freedom. If a theory can be formulated in terms of massive degrees of freedom, the light-cone vacuum is therefore trivially empty. Usually it is possible to achieve this situation in gauge theories by applying high-energy cut-offs.¹

In the Schrodinger picture, a stable relativistic boundstate (such as a hadron) can be represented as a state $|\psi(P)\rangle$ at a particular canonical time, which is an eigenvector of the Hamiltonian generator of time evolution. In light-cone quantisation, $|\psi(P)\rangle$ is an eigenvector of P^- , defined at $x^+ = \text{constant}$, and is labelled by momenta (P^+, \mathbf{P}) . It can be expanded in the light-cone Fock space of its parton constituents. An important consideration is the extent to which this expansion converges, since in a highly relativistic system particle production can be copious. If the Fock space amplitude is denoted $\psi_n(x_i, \mathbf{k}_i, s_i)$ for n partons carrying longitudinal momentum fractions $x_i = k_i^+/P^+$, transverse momenta \mathbf{k}_i , and helicities s_i , then

$$|\psi(P)\rangle = \sum_n \int \left[\prod_{i=1}^n d^2\mathbf{k}_i dx_i \right] \delta\left(1 - \sum_i x_i\right) \delta\left(\mathbf{P} - \sum_i \mathbf{k}_i\right) \sum_{s_i} \psi_n(x_i, \mathbf{k}_i, s_i) |n; x_1, \mathbf{k}_1, s_1, \dots, x_n, \mathbf{k}_n, s_n\rangle. \quad (26)$$

The multi-parton structure of this wavefunction is much simpler than in other quantization schemes. As indicated above, one can choose high-energy cut-offs such that it contains no disconnected vacuum contributions. The convergence with n of the Fock expansion Eq. (26) is usually very fast in this case for low-mass states $|\psi(P)\rangle$. The parton constituents appearing in Eq. (26) are on their mass shell

$$k_i^- = \frac{\mathbf{k}_i^2 + m_i^2}{2k_i^+} \quad (27)$$

but off the light-cone energy shell $P^- < \sum_i k_i^-$. Since $P^+ = \sum_i k_i^+$ and $\mathbf{P} = \sum_i \mathbf{k}_i$, the light-cone energy of a Fock state contribution typically rises like the square of the number of constituents rather than the number of constituents. The lowest energy boundstates are then dominated by just a few constituents.

In order to take advantage of these special properties of light-cone coordinates in the description of hadrons, it is necessary to formulate QCD in a light-cone Hamiltonian framework. In this review, we are going to outline the concept of the transverse lattice regulator, which is tailored to suit the manifest symmetries of the light-cone framework. As in other lattice gauge theories, this high-energy cut-off naturally exhibits linear confinement in the bare Hamiltonian. It will also facilitate the introduction of massive elementary degrees of freedom. The rapid convergence of the Fock space expansion in constituents is explicitly realised (for the pure glue theory at least). A number of illustrative applications to the boundstate physics of glueballs, light and heavy mesons will be given.

1.2 Physical motivation for light-cone framework

The physical origin of interest in light-cone formulations of quantum field theory can be traced to the fact that many high-energy scattering experiments probe hadron structure exceedingly close to the light-cone. For example, in deep inelastic electron-nucleon scattering experiments (DIS) one measures

¹A caveat involving the light-cone gauge fixing is described later.

the inclusive cross section (Fig. 1)

$$\frac{d^2\sigma}{dE'd\Omega} = \frac{\alpha^2}{4E^2 \sin^4 \frac{\theta}{2}} \left[W_2(Q^2, \nu) \cos^2 \frac{\theta}{2} + 2W_1(Q^2, \nu) \sin^2 \frac{\theta}{2} \right], \quad (28)$$

where P is the momentum of the nucleon before the scattering, q is the momentum transfer, ν is the energy transfer in the lab frame, θ the lepton scattering angle in this frame and E, E' the lepton initial and final energies.

Since the momentum transfer is always space-like in these experiments, it is convenient to introduce $Q^2 = -q^2 > 0$. The functional dependence on the kinematical variables in Eq. (28) is the most general one permitted by Lorentz invariance. In general $W_{1,2}(Q^2, \nu)$ are complicated functions of two variables (Q^2 and ν) which parameterize the non-trivial structure of the nucleon target. However, in the Bjorken limit, where both the momentum transfer $Q^2 \equiv -q^2$ and the energy transfer $P \cdot q \equiv M\nu$ become very large, such that $x_{Bj} = \frac{Q^2}{2M\nu}$ stays finite, where M is nucleon mass, one finds that the structure functions satisfy approximate ‘scaling’

$$MW_1(Q^2, \nu) \approx F_1(x_{Bj}) \quad \nu W_2(Q^2, \nu) \approx F_2(x_{Bj}). \quad (29)$$

These scaling functions F_i probe light-like correlations in the target. To see this, one first uses the optical theorem to relate the inclusive lepton-hadron cross section to the imaginary part of the forward Compton amplitude (Fig. 1). In the Bjorken limit, only those contributions to the forward Compton amplitude survive where the incoming and the outgoing photons couple to the same quark line. All other contributions are suppressed because they require the exchange of additional gluons to route the large momentum from the incoming photon to the outgoing photon. This is the physics reason for the dominance of so called ‘handbag diagrams’ in DIS (Fig. 2).

Asymptotic freedom implies that one can neglect final state interactions of the struck quark in DIS. Applied to the forward Compton amplitude, this means that one can neglect interactions of the ‘hard’ quark which transfers the momentum in the handbag diagram. Finally, being a high-energy quark, this ‘active’ quark in DIS moves with nearly the speed of light in a direction prescribed by the kinematics of the scattering event (Fig. 3). Since the struck quark does not interact², it is as if the quark had been removed from the target at one space time point and is then replaced at another space time point displaced by a light-like distance. It should thus not come as a surprise that the physics which the parton distributions Eq. (29) probe is related to light-like correlation functions of quark fields of the form

$$\langle \psi(P) | \bar{\psi}_\alpha(0, \mathbf{x}) \psi_\beta(x^-, \mathbf{x}) | \psi(P) \rangle, \quad (30)$$

where $|\psi(P)\rangle$ is the target state. The ‘3’ direction in this case is the direction of the space component of the momentum transfer in the rest frame of the target. The first important ramification of these simple observations is that only in the light-cone framework can one express parton distributions probed in DIS as a ground state property of the nucleon. In all other frames the light-like correlation function Eq. (30) involves correlations in the time direction and therefore knowledge of the ground state wavefunction of the target is not sufficient to describe parton distributions — one also needs to know the time evolution of the target with one quark replaced by a quark that moves with nearly the speed of light along a straight line.

² This is strictly true in light-cone gauge $A^+ = 0$. In other gauges, the interaction of the struck quark is described by a ‘Glauber phase factor’, which can be identified with a straight line gauge string.

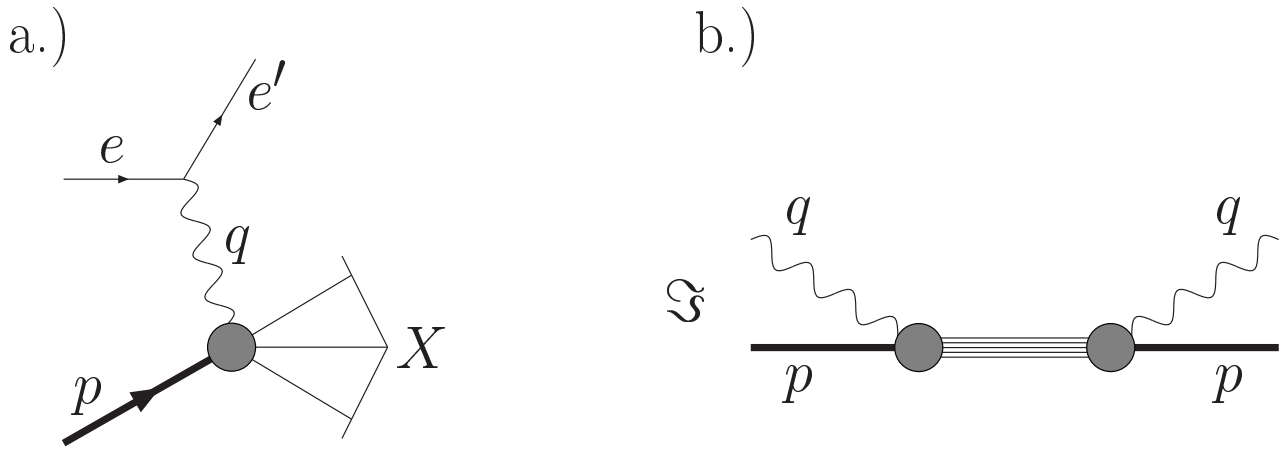


Figure 1: a.) Deep inelastic lepton-hadron scattering. X represents an arbitrary (unmeasured) hadronic final state. The inclusive cross section can be expressed in terms of the imaginary part of the forward Compton amplitude b.).

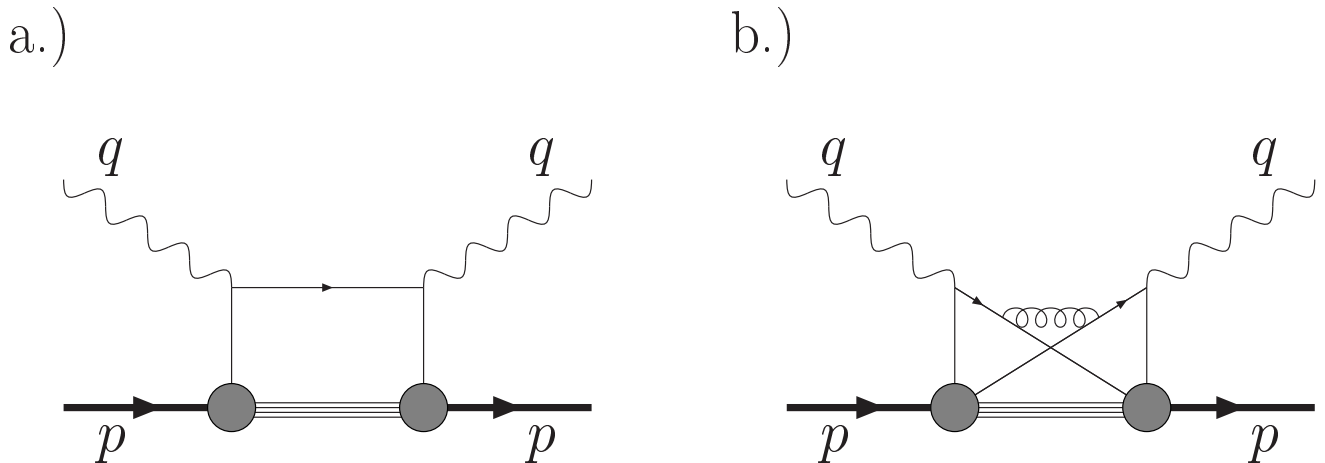


Figure 2: Contributions to the forward Compton amplitude where the two virtual photons couple to a.) the same quark ('handbag' diagram), b.) different quarks ('cat's ears' diagram). Diagrams where the two photons couple to different quarks require at least one additional hard gluon exchange in order to route the large momentum q from the incoming to the outgoing photon-quark vertex.

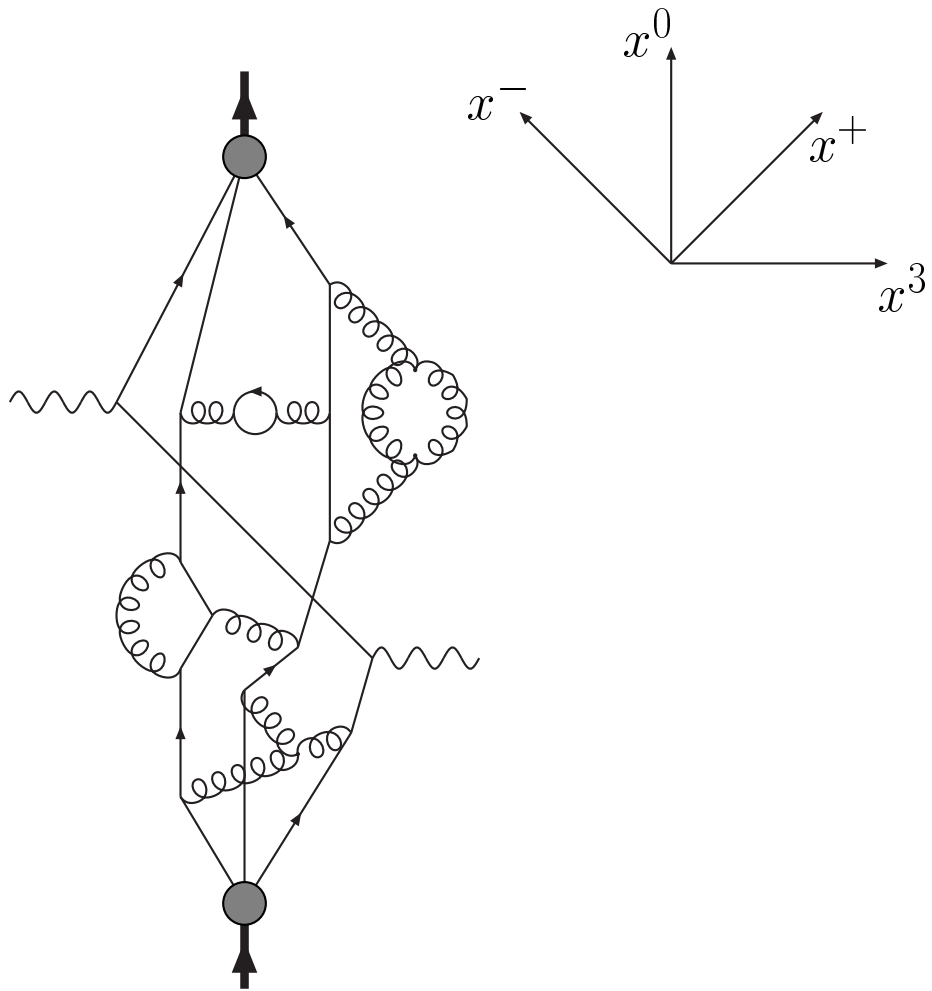


Figure 3: Space-time cartoon illustrating Compton scattering in the Bjorken limit, where the struck quark propagates without interactions along a light-like direction.

In terms of the Fock expansion (26), the parton distribution function is defined as

$$q(x) = \sum_n \int \left[\prod_{i=1}^n dx_i d^2\mathbf{k}_i \right] \delta\left(1 - \sum_i x_i\right) \delta\left(\mathbf{P} - \sum_i \mathbf{k}_i\right) \sum_{s_i} |\psi_n(x_i, \mathbf{k}_i, s_i)|^2 \sum_j \delta(x - x_j), \quad (31)$$

where the \sum_j extends over quarks with flavor q . Then

$$2F_1(x) = \frac{F_2(x)}{x} = \sum_q e_q^2 q(x) \quad (32)$$

for electric charges e_q of flavour q . In all other frames there is no such simple interpretation of structure functions and one has to use less direct methods to compute parton distributions (e.g. in Euclidean lattice gauge theory one calculates moments and inverts the moment expansion).

Although DIS is perhaps the most prominent example of the applications of the light-cone framework, there are many other examples for high-energy scattering experiments where light-cone coordinates play a distinguished role. The underlying physics reason why they play such a role is the simple fact that constituents travel along a nearly light-like direction after receiving a high energy-momentum transfer.

2 Pure transverse lattice gauge theory

2.1 Colour-dielectric formulation of the light-cone Hamiltonian

In this section, we discuss the ideas that lead one to tackle light-cone Hamiltonian quantization of gauge theories with a lattice cut-off. We outline some of the possible approaches to their construction. Particular attention will be paid to a method — the colour-dielectric formulation — that has led to a number of explicit results in hadronic physics, and which are described in more detail later. We begin with pure gauge theories, leaving the treatment of fermions on the transverse lattice to section 4.

To proceed to the solutions of a quantum field theory, with its continuously infinite degrees of freedom, one must put kinematical cut-offs or other restrictions on the Hilbert space. To remove the errors this introduces, one may then extrapolate these cut-offs, provided a continuum limit exists, or renormalise observables to account for degrees of freedom above the cut-off. Often one does both of these things, with an approximate renormalisation at a given cut-off designed to improve convergence of the extrapolation. Alternatively, instead of extrapolating the cut-off, one may try to do a systematically better approximate renormalisation at a given cut-off, for example by allowing gradually more complicated forms for renormalised operators appearing in observables.

For the study of QCD, we take the view that some residual gauge invariance, left over after any gauge fixing and imposition of cut-offs, is probably essential to produce generic linear confinement. By ‘generic’, we mean before any renormalisation of couplings and/or extrapolation to the continuum limit has been made. In this way, even a zeroth approximation to the cut-off gauge theory will automatically produce strong interaction physics close to that of the real world. A lattice cut-off is one means of retaining the required residual gauge invariance [10, 11].

For the purposes of Hamiltonian quantization, one must have a continuous time direction. In the case of light-cone Hamiltonian quantization, in addition to continuous light-cone time x^+ , light-cone space x^- should not have a short distance cut-off either. This is because x^- is conjugate to p^+ and

a large p^+ cut-off excludes small not large light-cone energies p^- , and therefore artefacts introduced by a lattice in x^- do not necessarily disappear in the formal continuum limit [3]. Furthermore, it is necessary to keep the x^- direction continuous if one wants to preserve the manifest boost invariance in one direction, which is one of the advantages of the light-cone formulation. Therefore, at most we can impose a lattice cut-off on transverse directions. The transverse lattice was suggested by Bardeen and Pearson [1], shortly after the discovery of lattice gauge theories. We will leave the question about how to cut off large x^- until later.

In 3+1 spacetime dimensions we introduce a square lattice of spacing a in the ‘transverse’ directions $\mathbf{x} = \{x^1, x^2\}$ and a continuum in the $\{x^0, x^3\}$ directions. $SU(N)$ gauge field degrees of freedom are represented by continuum Hermitian gauge potentials $A_\alpha(\mathbf{x}, x^+, x^-)$ and $N \times N$ link matrices $M_r(\mathbf{x}, x^+, x^-)$. $A_\alpha(\mathbf{x})$ resides on the plane $\mathbf{x} = \text{constant}$, while $M_r(\mathbf{x})$ is associated with a link from \mathbf{x} to $\mathbf{x} + a\hat{\mathbf{r}}$, where $\hat{\mathbf{r}}$ is a unit vector in direction r . $M_r(\mathbf{x})^\dagger$ goes from $\mathbf{x} + a\hat{\mathbf{r}}$ to \mathbf{x} . These variables map under transverse lattice gauge transformations $U(\mathbf{x}, x^+, x^-) \in SU(N)$ as

$$\begin{aligned} A_\alpha(\mathbf{x}) &\rightarrow U(\mathbf{x})A_\alpha(\mathbf{x})U^\dagger(\mathbf{x}) + i(\partial_\alpha U(\mathbf{x}))U^\dagger(\mathbf{x}) \\ M_r(\mathbf{x}) &\rightarrow U(\mathbf{x})M_r(\mathbf{x})U^\dagger(\mathbf{x} + a\hat{\mathbf{r}}) . \end{aligned} \quad (33)$$

The simplest gauge-covariant combinations are M_r , $F_{\alpha\beta} = \partial_\alpha A_\beta - \partial_\beta A_\alpha - i[A_\alpha, A_\beta]$, $\det M_r$, $\overline{D}^\alpha M_r$, etc., where the covariant derivative is

$$\overline{D}_\alpha M_r(\mathbf{x}) = (\partial_\alpha + iA_\alpha(\mathbf{x})) M_r(\mathbf{x}) - iM_r(\mathbf{x})A_\alpha(\mathbf{x} + a\hat{\mathbf{r}}) . \quad (34)$$

Note that M itself need not be restricted to $SU(N)$, although it is necessary to do so when approaching the transverse continuum limit $a \rightarrow 0$.

If we do limit ourselves to $M \in SU(N)$, the simplest transverse lattice action that can produce the correct continuum limit is

$$\begin{aligned} A = & \sum_{\mathbf{x}} \int dx^+ dx^- - \frac{a^2}{2g^2} \text{Tr}\{F^{\alpha\beta} F_{\alpha\beta}\} + \frac{1}{g'^2} \sum_r \text{Tr}\{\overline{D}_\alpha M_r(\mathbf{x})(\overline{D}^\alpha M_r(\mathbf{x}))^\dagger\} \\ & + \frac{1}{2g''^2 a^2} \sum_{r \neq s} \left(\text{Tr}\{M_r(\mathbf{x})M_s(\mathbf{x} + a\hat{\mathbf{r}})M_r^\dagger(\mathbf{x} + a\hat{\mathbf{s}})M_s^\dagger(\mathbf{x})\} - 1 \right) . \end{aligned} \quad (35)$$

As the lattice spacing a is taken to zero, the interaction terms will select smooth configurations as the dominant contributions to the quantum path integral; both the interactions mediated by the local two-dimensional gauge fields A_α and the plaquette interactions g'' will generate large potentials, unless the link configurations are smooth. Inserting the Bloch-wave expansion

$$M_r(\mathbf{x}) = \exp [iaA_r(\mathbf{x} + a\hat{\mathbf{r}}/2)] , \quad (36)$$

and displaying only the lowest order contributions in powers of a , one obtains

$$\begin{aligned} A = & - \int dx^0 dx^3 \sum_{\mathbf{x}} \frac{a^2}{2g^2} \text{Tr}\{F^{\alpha\beta} F_{\alpha\beta}\} + \frac{a^2}{2g'^2} \text{Tr}\{F^{\alpha r} F_{\alpha r} + F^{r\alpha} F_{r\alpha}\} \\ & + \frac{a^2}{2g''^2} \text{Tr}\{F^{rs} F_{rs}\} + O(a^4) . \end{aligned} \quad (37)$$

Tuning $g = g' = g''$ yields the Lorentz-invariant classical continuum limit. In deriving Eq. (37), the fields $A_{\pm}(\mathbf{x})$ were also assumed to be slowly varying on the lattice.

From Eq. (35), we see that the basic action for each link on the transverse lattice is the two-dimensional unitary $SU(N)$ principal chiral non-linear sigma model. The models are gauged and connected to one another through the plaquette interaction and the covariant derivative Eq. (34). In an ideal world, there would be an exact solution to the primary chiral sigma model, which could be used as a kernel to solve the entire theory perturbatively in the interactions. The idea would be to use the states that are diagonal with respect to the two-dimensional non-linear sigma model Hamiltonian as a basis for construction of the gauge-singlet bound states of the full higher-dimensional theory. Griffin [12] has suggested that by introducing Wess-Zumino [13] terms into the sigma model action, the non-linear dynamics can be studied in the basis of (linear) currents given by the well-studied and exactly solvable Wess-Zumino-Witten (WZW) model [14]. The Wess-Zumino terms in the action will become irrelevant operators, suppressed by powers of a , in the transverse continuum limit. Although promising, the technical details of carrying through this approach [15] have proved sufficiently formidable that no realistic calculations have yet been performed.

If we relax the $SU(N)$ constraint, allowing the link variables M to be general complex matrices, we must add to the action Eq. (35) a gauge-invariant potential $V(M)$, with the minimal requirement that it constrains M to the $SU(N)$ group manifold as $a \rightarrow 0$. The study of such linearized, or ‘colour-dielectric’ lattice gauge theories at finite a has some history in the case of four-dimensional Euclidean lattices; we refer to the review of Pirner [16]. Physically, linearized variables M may be thought of as being obtained by a smearing of all flux lines over paths \mathcal{C} between two points $(\mathbf{x}, \mathbf{x} + a\hat{\mathbf{r}})$, with some weight $\rho(\mathcal{C})$;

$$M_r(\mathbf{x}) = \sum_{\mathcal{C}} \rho(\mathcal{C}) \text{P exp} \left\{ i \int_{\mathcal{C}} A_{\mu} dx^{\mu} \right\} . \quad (38)$$

Different weights give rise to different potentials $V(M)$, related by reparameterization invariance. A simple potential that produces the correct $a \rightarrow 0$ behaviour is

$$V(M) = \frac{N}{\lambda} \left(\text{Tr} \left\{ (1 - M_r^{\dagger}(\mathbf{x}) M_r(\mathbf{x}))^2 \right\} + (\det M - 1)^2 \right) , \quad (39)$$

where $\lambda \rightarrow 0$ as $a \rightarrow 0$. However, it is not equivalent to a smeared continuum theory when λ is finite — such a potential would be infinitely more complicated. Now we deal with two-dimensional *linear* sigma models at each \mathbf{x} and, provided $M = 0$ is the groundstate, a simple basis for solving the full four-dimensional theory presents itself. However, it is easy to see that any $V(M)$ with the correct $a \rightarrow 0$ properties will have a tachyonic mass term for M near this limit. The non-trivial vacuum structure that must be present to stabilize the groundstate severely complicates matters, particularly in light-cone quantization. One may perform quantization of the lattice theory with couplings chosen so that $M = 0$ is the groundstate, but one cannot approach the usual continuum limit in this case.

At this point, it is worth recalling what is known about Euclidean colour-dielectric lattice gauge theory. If the link matrix M on a 4-dimensional Euclidean lattice is not tachyonic, a ‘strong coupling’ expansion of the path integral about $M = 0$ may be performed [17]. Mack has shown that a colour-dielectric picture of confinement results [18, 19]. Accordingly, we shall refer to this as the *colour-dielectric regime*. Moreover, there is evidence for $SU(2)$ that the partition function, subject to ‘block-spin’ transformations, has renormalisation group trajectories which pass into the colour-dielectric regime at short enough correlation length [16]. Therefore, the picture one should keep in mind is the following.

Suppose one decomposes $M = HU$ into a Hermitian matrix H and a unitary matrix U . As the continuum limit $a \rightarrow 0$ is approached, $H = H_0 + \tilde{H}$ gets a VEV H_0 , while the fluctuation \tilde{H} becomes very heavy and decouples. Near the continuum limit, H_0 appears in the equations of motion like a generalised dielectric constant [18]. In this regime the field M is tachyonic. As the lattice spacing a is increased, scaling trajectories may push one into a region of positive mass squared for M , where H_0 vanishes and \tilde{H} is fully dynamical. The mass of M then increases with a . This suggests it may be possible to obtain results relevant to the continuum limit by studying the colour-dielectric regime. The more detailed investigation of this idea on the transverse lattice will be presented later. In the remainder of this section we will set up the details of the light-cone quantization on the transverse lattice, with potentials $V(M)$ chosen so that $M = 0$ is the minimum.

For definiteness, consider the Lagrangian

$$L = \sum_{\mathbf{x}} \int dx^- - \frac{1}{2G^2} \text{Tr}\{F^{\alpha\beta}F_{\alpha\beta}\} - U_{\mathbf{x}}(M) + \sum_r \text{Tr}\{\bar{D}_\alpha M_r(\mathbf{x})(\bar{D}^\alpha M_r(\mathbf{x}))^\dagger\} , \quad (40)$$

where

$$U_{\mathbf{x}}(M) = \mu_b^2 \sum_r \text{Tr}\{M_r(\mathbf{x})M_r^\dagger(\mathbf{x})\} - \frac{\beta}{Na^2} \sum_{r \neq s} \text{Tr}\{M_r(\mathbf{x})M_s(\mathbf{x} + a\hat{\mathbf{r}})M_r^\dagger(\mathbf{x} + a\hat{\mathbf{s}})M_s^\dagger(\mathbf{x})\} . \quad (41)$$

Since M is now a linear variable, we are free to rescale it so that it has a canonically normalised kinetic term. We will choose μ_b^2 sufficiently large that we may quantize about $M_r = 0$.

The gauge invariance is partially fixed by setting $A_- = 0$. This axial gauge allows us to construct a Hilbert space of positive norm states that is diagonal in light-cone momentum space. A_+ then satisfies a constraint equation of motion, which can be used to eliminate it at the classical level;

$$(\partial_-)^2 A_+ = \frac{G^2}{2} \left(J^+ - \frac{1}{N} \text{Tr} J^+ \right) , \quad (42)$$

$$J^+(\mathbf{x}) = i \sum_r \left(M_r(\mathbf{x}) \overset{\leftrightarrow}{\partial}_- M_r^\dagger(\mathbf{x}) + M_r^\dagger(\mathbf{x} - a\hat{\mathbf{r}}) \overset{\leftrightarrow}{\partial}_- M_r(\mathbf{x} - a\hat{\mathbf{r}}) \right) . \quad (43)$$

Introducing gauge indices $\{i, j \in \{1, 2, \dots, N\}\}$, the canonical momenta are found to be $\pi_{ij}(M_r) = \partial_- M_{r,ij}^*$. It is then straightforward to canonically derive the generators of translations in x^+ and x^- . At time $x^+ = 0$ these are respectively

$$P^- = \int dx^- \sum_{\mathbf{x}} \frac{G^2}{4} \left(\text{Tr} \left\{ J^+ \frac{1}{(i\partial_-)^2} J^+ \right\} - \frac{1}{N} \text{Tr}\{J^+\} \frac{1}{(i\partial_-)^2} \text{Tr}\{J^+\} \right) + U_{\mathbf{x}}(M) \quad (44)$$

$$P^+ = \int dx^- \sum_{\mathbf{x}, s} 2 \text{Tr}\{\partial_- M_s(\mathbf{x})\partial_- M_s(\mathbf{x})^\dagger\} \quad (45)$$

P^- is the light-cone Hamiltonian. Of course, the transverse translation generator \mathbf{P} does not exist because of the short-distance lattice cut-off on \mathbf{x} . It is nevertheless possible to construct states boosted in the transverse direction, since at time $x^+ = 0$ one may canonically derive the further light-cone generators

$$M^{-+} = \int dx^- \sum_{\mathbf{x}, s} x^- 2 \text{Tr}\{\partial_- M_s(\mathbf{x})\partial_- M_s(\mathbf{x})^\dagger\} , \quad (46)$$

$$M^{+r} = - \int dx^- \sum_{\mathbf{x}, s} 2 \left(x^r + \frac{a}{2} \delta^{rs} \right) \text{Tr}\{\partial_- M_s(\mathbf{x})\partial_- M_s(\mathbf{x})^\dagger\} . \quad (47)$$

For the last expression, the transverse co-ordinate of a link has by convention been taken at the centre of the link. M^{-+} generates boosts in the x^- direction, while M^{+r} is a combination of boost in the x^r direction and rotation [9].

2.2 Determination of Fock space eigenfunctions

In the quantum theory, commutation relations at fixed x^+ are

$$\left[M_{r,ij}(x^-, \mathbf{x}), \partial_- M_{s,kl}^*(y^-, \mathbf{y}) \right] = \frac{i}{2} \delta_{ik} \delta_{jl} \delta(x^- - y^-) \delta_{\mathbf{xy}} \delta_{rs} . \quad (48)$$

A convenient Fock space representation employs longitudinal momentum space but transverse position space;

$$M_r(x^+ = 0, x^-, \mathbf{x}) = \frac{1}{\sqrt{4\pi}} \int_0^\infty \frac{dk^+}{\sqrt{k^+}} \left(a_{-r}(k^+, \mathbf{x}) e^{-ik^+x^-} + a_r^\dagger(k^+, \mathbf{x}) e^{ik^+x^-} \right) , \quad (49)$$

$$\left[a_{\lambda,ij}(k^+, \mathbf{x}), a_{\rho,kl}^*(\tilde{k}^+, \mathbf{y}) \right] = \delta_{ik} \delta_{jl} \delta_{\lambda\rho} \delta_{\mathbf{xy}} \delta(k^+ - \tilde{k}^+) , \quad (50)$$

$$\left[a_{\lambda,ij}(k^+, \mathbf{x}), a_{\rho,kl}(\tilde{k}^+, \mathbf{y}) \right] = 0 . \quad (51)$$

Here, λ and $\rho \in \{\pm 1, \pm 2\}$, $a_{\lambda,ij}^* = a_{\lambda,ji}^\dagger$. We define a Fock vacuum state via $a_{\lambda,ij}|0\rangle = 0 \forall \lambda, i, j$. The operator $a_{r,ij}^\dagger(k^+, \mathbf{x})$ then creates a link-parton with longitudinal momentum k^+ , carrying colour i at \mathbf{x} to j at $\mathbf{x} + a\hat{\mathbf{r}}$, while $a_{-r,ij}^\dagger(k^+, \mathbf{x})$ creates a link with opposite orientation. This Fock space is diagonal in P^+ Eq. (45) and serves as a basis for finding the eigenvalues of the matrix P^- .

The only infinite renormalisations required in P^- come from normal-orderings due to infinite self-energies. Here we may follow the same procedure as in two-dimensional gauge theories [20, 21, 22, 23]. With normal-ordered currents J^+ , the current-current interaction in Eq. (44) produces linear and logarithmically divergent self-energies

$$\frac{\bar{G}^2}{4\pi} \int_0^\infty \frac{dp^+}{p^+} + \frac{\bar{G}^2}{\pi} \int_0^{k^+} dp^+ \frac{k^+}{(k^+ - p^+)^2} , \quad (52)$$

where $\bar{G} = G\sqrt{(N^2 - 1)/N}$ with the dimensions of mass. The logarithmic divergence may be absorbed by a renormalisation $\mu_b^2 \rightarrow \mu_R^2$. The linear divergence must be retained to cancel a similar divergence appearing at small momentum transfer [20]. With this prescription, the Fock vacuum is also the physical vacuum $P^+|0\rangle = P^-|0\rangle = 0$, provided we may neglect $k^+ = 0$ modes. Since the quadratic term in $U_{\mathbf{x}}(M)$ (see Eq. (41)) contributes energy μ_R^2/k^+ for each mode of momentum k^+ , it follows that zero modes of link fields with $\mu_R^2 > 0$ have infinite energy and decouple from physical states. This is the transverse lattice version of the colour-dielectric regime — a Fock space expansion about $M_r = 0$ is energetically justified.

The charges $\tilde{J}^+(0, \mathbf{x}) = \int dx^- J^+(x^-, \mathbf{x})$ are the generators of residual x^- -independent gauge symmetries. From the singular behaviour of P^- Eq. (44), one sees that the energy of a Fock state cannot be finite unless it is annihilated by $\tilde{J}^+(0, \mathbf{x})$ for any \mathbf{x} . This is the light-cone version of the Gauss law constraint (see Eq. (42)), which forces the net flux into any point to be zero [1]. The basis of finite-energy Fock states are thus global gauge singlets, such as

$$\text{Tr} \left\{ a_{-1}^\dagger(k_1^+, \mathbf{x}) a_2^\dagger(k_2^+, \mathbf{x}) a_{-1}^\dagger(k_3^+, \mathbf{x} + a\hat{2} - a\hat{1}) a_{-2}^\dagger(k_4^+, \mathbf{x} - a\hat{1}) a_1^\dagger(k_5^+, \mathbf{x} - a\hat{1}) a_1^\dagger(k_6^+, \mathbf{x}) \right\} |0\rangle , \quad (53)$$

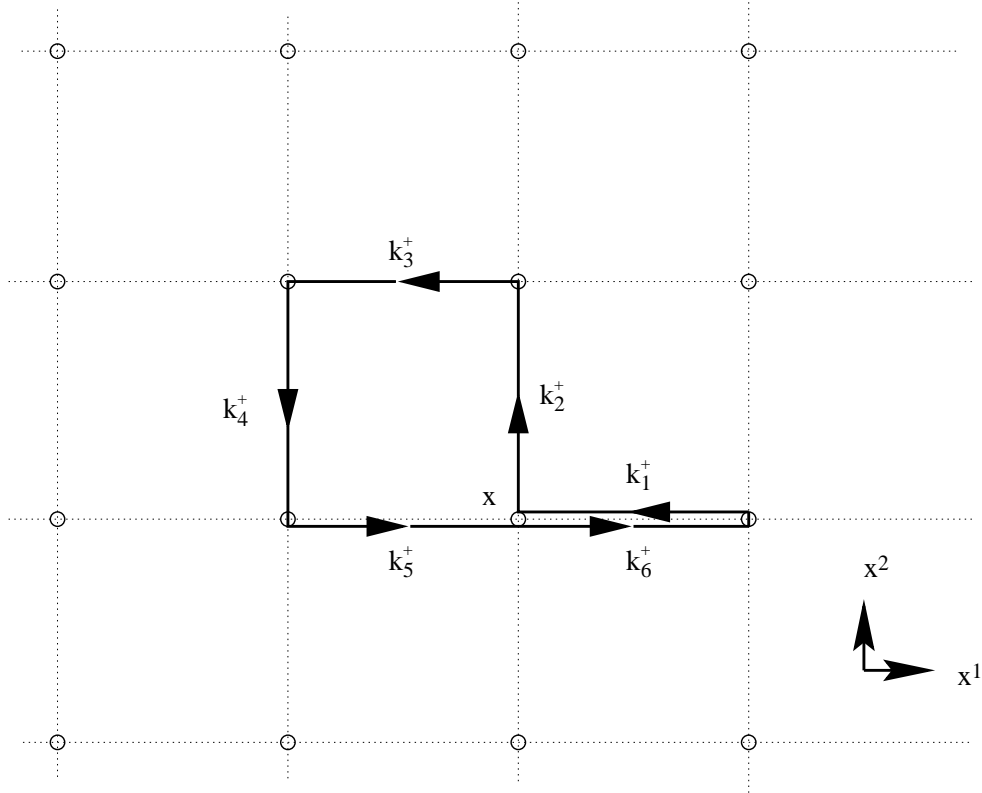


Figure 4: An example of a length-6 loop on the transverse lattice, showing also the longitudinal momentum carried by each link, corresponding to the Fock state Eq. (53).

as illustrated in Fig. 4. The longitudinal momenta k_m^+ are constrained to $\sum_{m=1}^6 k_m^+ = P^+$ in this example. Viewed in the position space (x^-, \mathbf{x}) , typical gauge singlets are illustrated in Fig. 5.

The transverse lattice theory possesses some discrete symmetries. There is charge conjugation

$$\mathcal{C} \left(a_{+r,ij}^\dagger(\mathbf{x})|0\rangle \right) = a_{-r,ji}^\dagger(\mathbf{x})|0\rangle . \quad (54)$$

There are two orthogonal reflection symmetries \mathcal{P}_r such that $P_r(x^s) = -\delta_{rs}x^s$ and

$$\mathcal{P}_r \left(a_{+r,ij}^\dagger(\mathbf{x})|0\rangle \right) = a_{-r,ij}^\dagger(P_r(\mathbf{x}) - a\hat{\mathbf{r}})|0\rangle . \quad (55)$$

The operation $\mathcal{P}_3(x^3) = -x^3$, and therefore the parity operator $\mathcal{P} = \mathcal{P}_3\mathcal{P}_2\mathcal{P}_1$, is more subtle in light-cone quantization since it is dynamical. On a set of p free particles of equal mass, the free particle limit of \mathcal{P}_3 acts as [24]

$$\mathcal{P}_3^{\text{free}} \left(\frac{k_m^+}{P^+} \right) = \left(k_m^+ \sum_{m'=1}^p \frac{1}{k_{m'}^+} \right)^{-1} . \quad (56)$$

This expression is sometimes useful for estimating the parity of a state, for example by tracking the state from the heavy particle limit, where $\mathcal{P}_3^{\text{free}}$ should coincide with \mathcal{P}_3 . 90-degree rotations $x^1 \rightarrow x^2$ are exact and can be used to distinguish the angular momentum projections $J_3 = 0, \pm 1, \pm 2$ from each other. Together these discrete symmetries form the group D_4 [22], with one-dimensional representations and a single two-dimensional irreducible representation. The one-dimensional representations corresponds

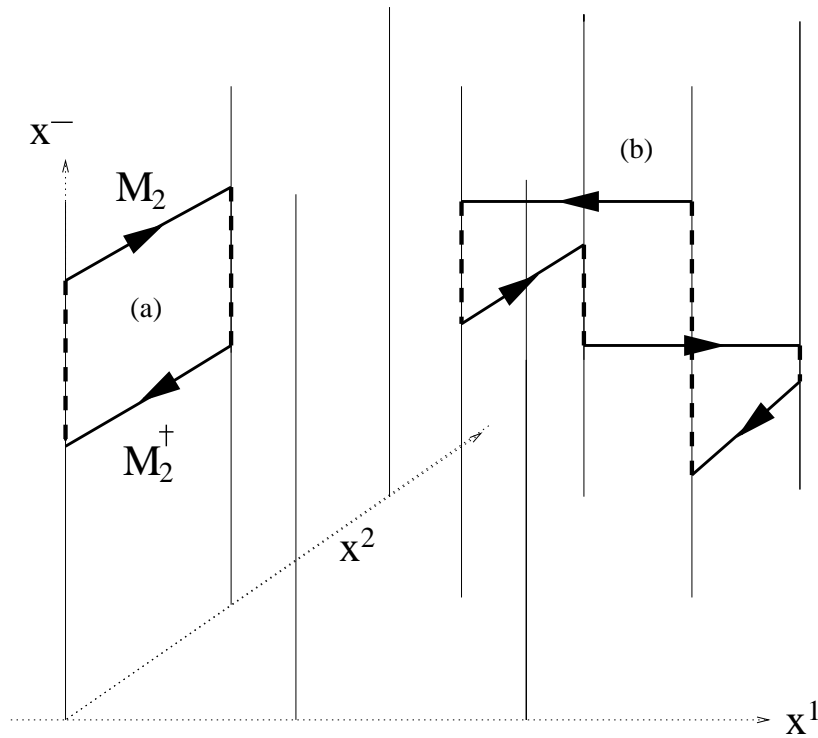


Figure 5: Gauge singlet configurations on the transverse lattice at fixed x^+ . Solid arrowed line represents a link matrix, chain dark lines represent $P \exp \int dx^- A_-$ insertions required for gauge invariance (these become trivial in $A_- = 0$ gauge).

to $J_3 = 0$ or symmetric and antisymmetric combinations of $J_3 = \pm 2$. The two-dimensional contains $J_3 = \pm 1$.

The simplest possible gauge-singlet Fock states consist of a link—anti-link pair (see Fig. 5(a)). A boundstate made from just these configurations can be written

$$|\psi(P^+)\rangle = \sum_{\mathbf{x}} \int_0^{P^+} \frac{dk_1 dk_2}{N} \delta(P^+ - k_1^+ - k_2^+) f_r(k_1^+/P^+, k_2^+/P^+) \text{Tr}\{a_r^\dagger(k_1^+, \mathbf{x}) a_{-r}^\dagger(k_2^+, \mathbf{x})\} |0\rangle. \quad (57)$$

$|\psi(P^+)\rangle$ is a $\mathbf{P} = 0$ state oriented in direction r . Let us use this subspace to illustrate the boundstate problem. We drop the index r , since it simply labels a doublet degeneracy, and introduce momentum fraction $x = k_1^+/P^+$. Projecting the eigenvalue equation $2P^+P^-|\psi(P^+)\rangle = \mathcal{M}^2|\psi(P^+)\rangle$ onto Fock basis states, one derives the following integral equation for individual Fock components [1]

$$\begin{aligned} \frac{\mathcal{M}^2}{G^2} f(x, 1-x) &= \left(\frac{m_b^2}{x} + \frac{m_b^2}{1-x} + \frac{1}{4\sqrt{x(1-x)}} \right) f(x, 1-x) \\ &+ \frac{1}{4\pi} \int_0^1 dy \frac{(x+y)(2-y-x)}{\sqrt{x(1-x)y(1-y)}} \left\{ \frac{f(x, 1-x) - f(y, 1-y)}{(y-x)^2} \right\}. \end{aligned} \quad (58)$$

\mathcal{M} is the invariant mass squared of the boundstate and $m_b = \frac{\mu_B}{G}$. The plaquette term β in Eq. (41) does not contribute in this subspace. We notice that the boundstate problem is equivalent in this case to that of two-dimensional QCD with complex scalar particles of matter [21, 23]. The spectrum of eigenvalues \mathcal{M} is infinite and discrete, corresponding to boundstate excitations of the double flux line connecting the adjoint scalars in the x^- direction. Eigenfunctions $f(x, 1-x)$ are of the form

$$f(x, 1-x) = x^\alpha (1-x)^\alpha P(x) \quad ; \quad \alpha \tan(\pi\alpha) = m_b^2, \quad (59)$$

such that $P(0) > 0$ and $P(1) > 0$. The endpoint index α is determined by consistency of the limit $x \rightarrow 0$ in Eq. (58), and is a simple example of a high-energy boundary condition for finite \mathcal{M} . The spectrum can be labelled by the number of zeros in $P(x)$. The groundstate is a symmetric function of x with no zeros; it has quantum numbers $|J_3|^{PC} = 0^{++}, 2^{++}$, where we use $\mathcal{P}^{\text{free}}$ to find \mathcal{P} . The first excited state has one zero and $J_3^{PC} = \pm 1^{+-}$. These states have some of the quantum numbers expected of the lightest glueballs, although the full wavefunction can be very different from that in the link—anti-link truncation of Fock space.

If we allow more links in Fock space (see Fig. 5(b) for example), the plaquette term β and the gauge kinetic term can now mix sectors differing by two links. This provides a mechanism for propagation of states on the transverse lattice. The wavefunction becomes more complicated than the form Eq. (57). As well as four- and higher-link components, the endpoint indices such as α get renormalised [25] (contrary to assumptions often made in the literature). It quickly becomes formidable to deal with an analytic basis of functions. As a result, most calculations with many particles have been performed with discrete numerical bases.

The transverse lattice does not completely regulate a light-cone quantum field theory because typically infra-red divergences appear in the x^- direction, after non-dynamical fields have been eliminated. This has been discussed earlier, concerning the current-current interaction $J^+(\partial_-)^{-2}J^+$ in Eq. (44) which contains a small k^+ singularity. Cutting out this region, the eigenvalues of the Hamiltonian can be made finite in the principle-value sense by including linearly-divergent self-energies [20].

Unfortunately, by putting a cut-off on small k^+ , by making x^- periodic for example [26], it appears impossible to eliminate or gauge away the $k^+ = 0$ modes of A_{\pm} . In fact, it is possible to gauge away the zero mode of A_+ at a particular x^+ , but the zero mode of A_- will always remain as a dynamical quantum-mechanical degree of freedom in Fock space [27]. There is some confusion in the literature as to how much this single mode can affect physical observables. A numerical estimate in ref.[28] claimed an effect for the spectrum of two-dimensional gauge theory with adjoint matter. Even here, it is not known to what extent the dynamics of the zero mode can be accounted for in renormalisation of existing couplings in the Hamiltonian. All transverse lattice calculations to date have made the approximation of explicitly omitting this zero mode from the Fock space.

Two basic techniques have been applied in the literature for performing Fock space calculations, which we now briefly describe. Both have their advantages and shortcomings. In general it is safest to use both methods, comparing results for consistency.

The first method uses a finite basis of wavefunctions $\psi_S(x_1, x_2, \dots, x_n)$, where S labels the shape in the transverse direction while x_i labels the P^+ momentum fraction carried by each link. The singular behaviour described above requires non-analytic behaviour of ψ when one or more of its arguments vanish. The simplest case has already been described when only the $n = 2$ sector is retained Eq. (57). A complete set of polynomials or trig functions would form a suitable basis for the analytic function $P(x)$ and, with the correct α , low-lying eigenfunctions converge rapidly in truncations of the basis. These forms are usually generalised to higher n for use in diagonalising the full Fock space Hamiltonian,

$$\psi_S(x_1, x_2, \dots, x_n) \sim x_1^\alpha x_2^\alpha \dots x_n^\alpha P(x_1, x_2, \dots, x_n) , \quad (60)$$

They have the advantage that all integrals can be performed analytically, using variations on the identity [22]

$$\int_0^1 dx dy \frac{[x(1-x)]^\alpha [y(1-y)]^\beta}{(x-y)^2} = -\frac{\alpha\beta}{2(\alpha+\beta)} B(\alpha, \alpha) B(\beta, \beta) \quad (61)$$

However, in general α becomes renormalised in all but the highest Fock state [25] and there is no simple analytic formula for it analogous to Eq. (57). Moreover, the factorized form Eq. (60) is incorrect at corners of phase space. When two or more momenta vanish, the wavefunction in general does not. With the incorrect endpoint behaviour, one may get slow convergence in the truncation of basis functions P , and an independent check is desirable.

An alternative basis uses the Discrete Light-Cone Quantization (DLCQ) [29]. This uses the fact that the Fock space splits up into disjoint sectors of fixed P^+ . By making $x^- = x^- + \mathcal{L}$ periodic with a momentum-dependent period $\mathcal{L} = 2\pi K/P^+$, for some integer K , parton momentum fractions k^+/P^+ take the form i/K for positive integers $i < K$, independent of \mathcal{L} . In other words, they are simply partitions of K , divided by K . For given K this produces a finite-dimensional approximation to the Fock space, and answers can be extrapolated to $K = \infty$. It is often expedient to take anti-periodic boundary conditions, so that $k^+/P^+ = j/2K$ where j is odd. This allows a better sampling of the small k^+ region, leading to faster convergence when observables are extrapolated in K . For example, at $K = 4$, the allowed colour-singlet states would be

$$\begin{aligned} & \{ \text{Tr} \{ a_1^\dagger(P^+/4) a_{-1}^\dagger(3P^+/4) \} |0\rangle, \text{Tr} \{ a_{-1}^\dagger(P^+/4) a_1^\dagger(3P^+/4) \} |0\rangle, \\ & \text{Tr} \{ a_2^\dagger(P^+/4) a_{-2}^\dagger(3P^+/4) \} |0\rangle, \text{Tr} \{ a_{-2}^\dagger(P^+/4) a_2^\dagger(3P^+/4) \} |0\rangle, \\ & \text{Tr} \{ a_1^\dagger(P^+/4) a_1^\dagger(P^+/4) a_{-1}^\dagger(P^+/4) a_{-1}^\dagger(P^+/4) \} |0\rangle, \text{Tr} \{ a_2^\dagger(P^+/4) a_2^\dagger(P^+/4) a_{-2}^\dagger(P^+/4) a_{-2}^\dagger(P^+/4) \} |0\rangle, \end{aligned}$$

$$\begin{aligned}
& \text{Tr} \{a_1^\dagger(P^+/4)a_2^\dagger(P^+/4)a_{-2}^\dagger(P^+/4)a_{-1}^\dagger(P^+/4)\}|0\rangle, \text{Tr} \{a_2^\dagger(P^+/4)a_1^\dagger(P^+/4)a_{-1}^\dagger(P^+/4)a_{-2}^\dagger(P^+/4)\}|0\rangle, \\
& \text{Tr} \{a_1^\dagger(P^+/4)a_{-2}^\dagger(P^+/4)a_2^\dagger(P^+/4)a_{-1}^\dagger(P^+/4)\}|0\rangle, \text{Tr} \{a_{-2}^\dagger(P^+/4)a_1^\dagger(P^+/4)a_{-1}^\dagger(P^+/4)a_2^\dagger(P^+/4)\}|0\rangle, \\
& \text{Tr} \{a_1^\dagger(P^+/4)a_2^\dagger(P^+/4)a_{-1}^\dagger(P^+/4)a_{-2}^\dagger(P^+/4)\}|0\rangle, \text{Tr} \{a_2^\dagger(P^+/4)a_1^\dagger(P^+/4)a_{-2}^\dagger(P^+/4)a_{-1}^\dagger(P^+/4)\}|0\rangle \}
\end{aligned}$$

The number of Fock states increases exponentially with K . This method has the advantage that it is easy to write down a basis and evaluate the interactions for many particles, without having to make any ansatz. However, because the discretization is not very sensitive to the small k^+ singularities in the interactions, convergence in K is quite slow. This can be partially overcome by using a continuous wavefunction basis for particles that interact and a DLCQ basis for spectators, when evaluating matrix elements of P^- . This improvement technique is described in refs.[30, 31].

So far we have considered states that are translationally invariant on the transverse lattice. States with non-zero \mathbf{P} may be obtained using the boost operator M_{-r} Eq. (47), whose action is

$$e^{-ib^r M_{-r}} a_\lambda^\dagger(k^+, \mathbf{x}) e^{ib^r M_{-r}} = a_\lambda^\dagger(k^+, \mathbf{x}) e^{-ik^+ \mathbf{b} \cdot (\mathbf{x} + a \text{Sgn}(\lambda) \hat{\lambda}/2)} ; \quad (62)$$

$$e^{-ib^r M_{-r}} |\psi(P^+, \mathbf{P})\rangle = |\psi(P^+, \mathbf{P} - \mathbf{b}P^+)\rangle . \quad (63)$$

In this way an arbitrary connected p -link state when boosted becomes

$$\sum_{\mathbf{y}} e^{i\mathbf{P} \cdot (\mathbf{y} + \bar{\mathbf{x}})} \text{Tr} \left\{ a_{\lambda_1}^\dagger(k_1^+, \mathbf{x}_1 + \mathbf{y}) a_{\lambda_2}^\dagger(k_2^+, \mathbf{x}_2 + \mathbf{y}) \cdots a_{\lambda_p}^\dagger(k_p^+, \mathbf{x}_p + \mathbf{y}) \right\} |0\rangle , \quad (64)$$

where

$$\sum_{i=1}^p \hat{\lambda}_i = 0 ; \quad \sum_{i=1}^p k_i^+ = P^+ ; \quad \bar{\mathbf{x}} = \frac{1}{P^+} \sum_{i=1}^p k_i^+ \left(\mathbf{x}_i + \frac{a \text{Sgn}(\lambda) \hat{\lambda}_i}{2} \right) . \quad (65)$$

Longitudinal boosts, generated by M_{-+} Eq. (46), simply rescale P^+ . For this reason it is often convenient to use boost-invariant P^+ momentum fractions.

2.3 Confinement of heavy sources

We now show how generic linear confinement arises in the transverse lattice theory in the colour-dielectric regime. An unambiguous criterion for this is provided by the potential between static colour sources [32]. We introduce a heavy scalar field $\phi(x^+, x^-, \mathbf{x})$ of mass ρ , in the fundamental representation of the gauge group, which is associated to lattice plane $\mathbf{x} = \text{constant}$. The simplest gauge invariant terms one can add to the action are

$$\sum_{\mathbf{x}} \int dx^- dx^+ (D_\alpha \phi)^\dagger D^\alpha \phi - \rho^2 \phi^\dagger \phi , \quad (66)$$

where

$$D_\alpha \phi = \partial_\alpha \phi + iA_\alpha \phi . \quad (67)$$

The heavy field contributes to the gauge current J^α in Eqn. (43) a new term

$$J_{\text{heavy}}^\alpha = -i (D^\alpha \phi) \phi^\dagger + i \phi (D^\alpha \phi)^\dagger . \quad (68)$$

Note that $\phi\phi^\dagger$ is an $N \times N$ colour matrix.

Let P^α represent the full 2-momentum of a system containing h heavy particles. It is convenient to split the full momentum into a ‘‘heavy’’ part plus a ‘‘residual’’ part P_{res}^α ,

$$P^\alpha = \rho h v^\alpha + P_{\text{res}}^\alpha, \quad (69)$$

where v^α is the covariant velocity of the heavy quarks, $v^\alpha v_\alpha = 1$. The full invariant mass squared (at $\mathbf{P} = 0$) is

$$\mathcal{M}^2 = 2P^+P^- = (h\rho)^2 + 2h\rho v^+P_{\text{res}}^- + 2P_{\text{res}}^+ (P_{\text{res}}^- + h\rho v^-) \quad (70)$$

The choice of v^+ is arbitrary and it is convenient to choose it such that $P_{\text{res}}^+ = 0$. Consequently, $v^+P_{\text{res}}^-$ is just the shift of the full invariant mass \mathcal{M} due to the interactions:

$$\mathcal{M} = h\rho + v^+P_{\text{res}}^- + O(1/\rho). \quad (71)$$

The minimum eigenvalue of the operator $v^+P_{\text{res}}^-$ is the usual energy associated with the heavy quark potential. It may be computed by extending Fock space to include the heavy sources. Define

$$\phi = \frac{1}{\sqrt{4\pi}} \int_{-\infty}^{\infty} \frac{dk}{\sqrt{\rho v^+ + k}} \left(b(k) e^{-iv_\alpha x^\alpha \rho - ikx^-} + d^\dagger(k) e^{iv_\alpha x^\alpha \rho + ikx^-} \right). \quad (72)$$

The $e^{iv_\alpha x^\alpha \rho}$ term removes an overall momentum ρv^α from the 2-momentum. Again, residual gauge invariance in $A_- = 0$ gauge leads to only singlet states having finite energy. As an example, let us construct a state with two co-moving infinitely heavy sources on the same site \mathbf{x} maintaining a fixed x^3 -separation L (this corresponds to an x^- separation of $2v^-L$):

$$|2\rangle = \frac{2\rho v^+}{\sqrt{N}} \int dx^- \phi^\dagger(x^+, x^- + Lv^-) \phi(x^+, x^- - Lv^-) |0\rangle e^{-2i\rho v_\alpha x^\alpha} \quad (73)$$

$$= \frac{1}{\sqrt{N}} \int_{-\infty}^{\infty} dk b^\dagger(k) d^\dagger(-k) e^{2iLv^-k}. \quad (74)$$

See Fig. 6(a). The associated energy shift is found to be

$$\frac{\langle 2|v^+P_{\text{res}}^-|2\rangle}{\langle 2|2\rangle} = \frac{\overline{G}^2 |L|}{4}. \quad (75)$$

Thus, we have linear confinement in this direction with squared string tension $\overline{G}^2/4$. Physically, it arises because the flux that passes between the heavy sources in this particular state cannot spread out in the transverse direction.

Sources separated in the transverse direction must be joined by a string of links, for gauge invariance (see Fig. 6(b) for a one-link example). It is easy to see that, for sufficiently wide transverse separation and large link mass m_b , the potential is dominated by the mass of the links forming this string, whose number will be minimized to form the potential. Each additional link increases the energy by $\overline{G}m_b$ and the separation of sources by a , leading to linear confinement with squared string tension $m_b\overline{G}/a$.

If we demand equivalence of the string tension $\sqrt{\sigma}$ in continuum and lattice directions, this is one method of fixing the lattice spacing a in units of \overline{G} . The full heavy-source calculation will involve fluctuations in the number of links. This will renormalise the string tensions in each direction. Unless

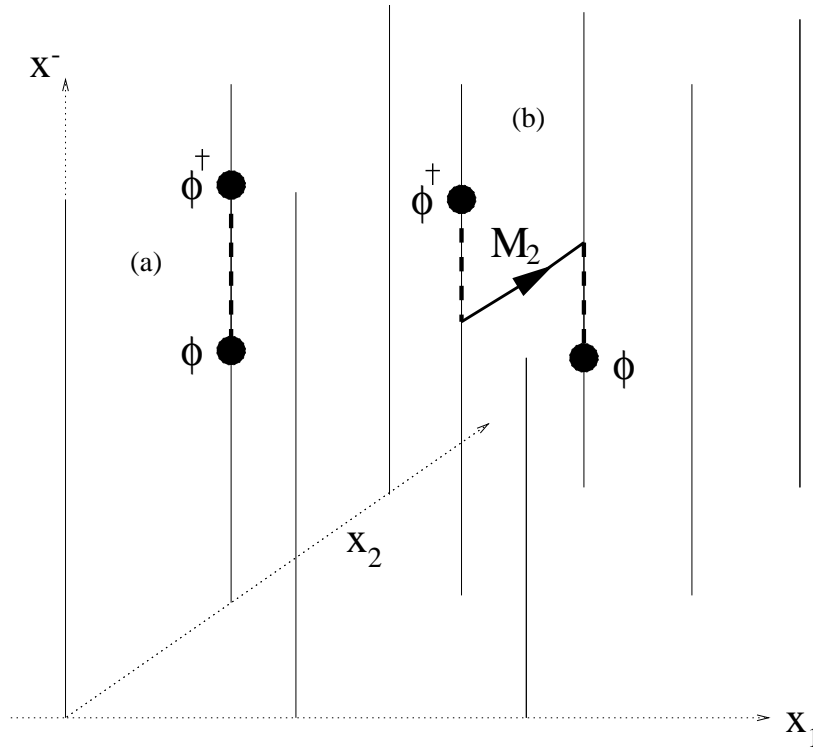


Figure 6: Gauge singlet configurations of fundamental representation sources ϕ and link fields M on the transverse lattice at fixed x^+ . Solid arrowed line represents a link matrix, chain dark lines represent $P \exp \int dx^- A_-$ insertions required for gauge invariance (these become trivial in $A_- = 0$ gauge).

some fine-tuning is performed, to completely screen the behaviour above by transverse fluctuations in the number of links, linear confinement will still be present.

Related to the heavy source calculations is the boundstate problem for winding modes that exist if we compactify transverse directions. By making the transverse lattice compact in direction r say

$$\mathbf{x} \equiv \mathbf{x} + a\hat{\mathbf{r}}D_r, \quad (76)$$

where D_r is the number of transverse links in direction r , we can construct a basis of Fock states that wind around these directions. For example

$$\text{Tr}\left\{a_{r_1}^\dagger(k_1^+, \mathbf{x}) a_{r_2}^\dagger(k_2^+, \mathbf{x} + a\hat{\mathbf{r}}_1) \cdots a_{r_p}^\dagger(k_p^+, \mathbf{x} + a\hat{\mathbf{r}}D_r - a\hat{\mathbf{r}}_p)\right\} |0\rangle \quad (77)$$

has winding number one in direction $\hat{\mathbf{r}}$. The mass spectrum of such winding modes rises linearly with D_r as $D_r \rightarrow \infty$. Unlike the potential between heavy sources, there are no ‘endpoint’ effects, and so the asymptotic linear rise should set in more quickly, especially for the groundstate in each D_r sector. Note that we cannot construct winding modes around a compactified x^3 as this clashes with the choice of light-cone coordinates.

2.4 Simplification in the Large N limit

It is well-known that gauge theories undergo considerable simplification in the limit of large N [33]. This is especially true of light-cone gauge theories, since the boundstate equation becomes a linear Schrödinger equation for connected loops of flux of the form $\text{Tr}\{a^\dagger a^\dagger \cdots a^\dagger\}$ [34]. Transitions to disconnected forms $\text{Tr}\{a^\dagger a^\dagger \cdots a^\dagger\} \cdot \text{Tr}\{a^\dagger a^\dagger \cdots a^\dagger\}$ are suppressed by $1/N$, as are interactions between non-sequential a^\dagger modes in the colour trace. Gauge singlet states involving the antisymmetric tensor $\epsilon_{i_1 \dots i_N}$ involve $O(N)$ links and therefore have infinite energy for sufficiently large link mass m_b . All this would also be true of other quantization schemes. However, in light-cone quantization with a trivial vacuum, there can be no creation or annihilation of loops of flux from the vacuum. Such processes, when allowed, are enhanced by powers of N , meaning that only in light-cone field theory does the leading order in $1/N$ evaluate connected amplitudes. This is illustrated in Fig. 7 for a loop-loop correlation, which is relevant for finding the spectrum of invariant masses \mathcal{M} . The corresponding boundstates, which are glueballs, are absolutely stable in the large- N limit.

Another simplification afforded by the large- N limit is Eguchi-Kawai reduction [35]. For the transverse lattice, this means that the light-cone Hamiltonian in the basis of $\mathbf{P} = \mathbf{0}$ Fock states is the same as the Hamiltonian for the corresponding problem where the transverse lattice is compactified on one link in each direction [36]. In other words, one makes the identification

$$M_r(\mathbf{x}) = M_r \quad \text{for all } \mathbf{x}. \quad (78)$$

in both basis states and Hamiltonian. For the basis states themselves, the identification Eq. (78) is obviously a one-one mapping. Any connected flux loop for a state of $\mathbf{P} = \mathbf{0}$ is completely specified by the sequence of orientations and longitudinal momenta of the link modes in the colour trace, and does not require knowledge of the absolute positions of the links on the lattice. In effect, large- N gauge theory has reduced to 1+1-dimensional large- N gauge theory with two complex matter fields in the adjoint representation. Powerful techniques developed in the study of two-dimensional field theory of this kind [37] can now be brought to bear on the problem.

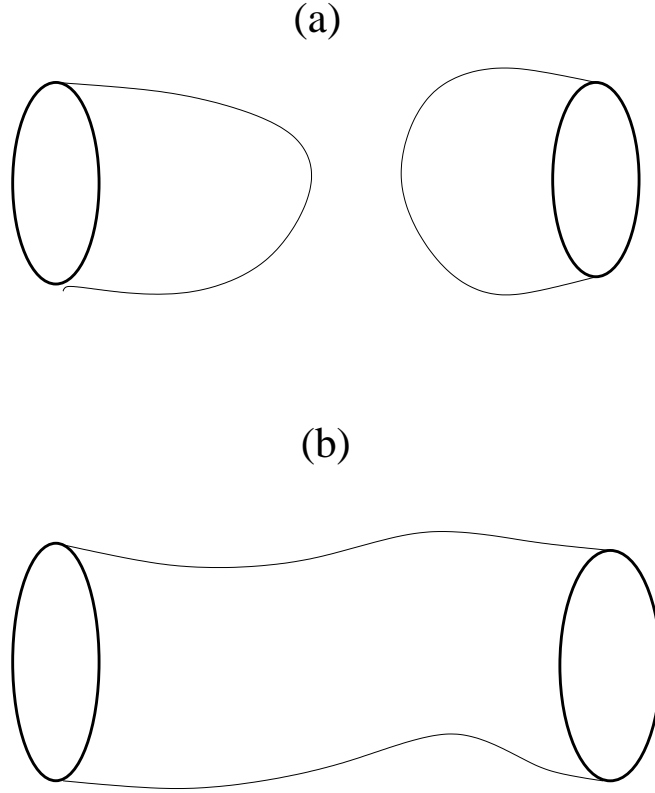


Figure 7: Worldsheet swept out by propagation of a flux loop (dark line). (a) The leading contribution $O(N^2)$, the disconnected amplitude, that is absent in light-cone quantization with a trivial vacuum. (b) Leading contribution $O(N^0)$ in light-cone quantization, the connected amplitude.

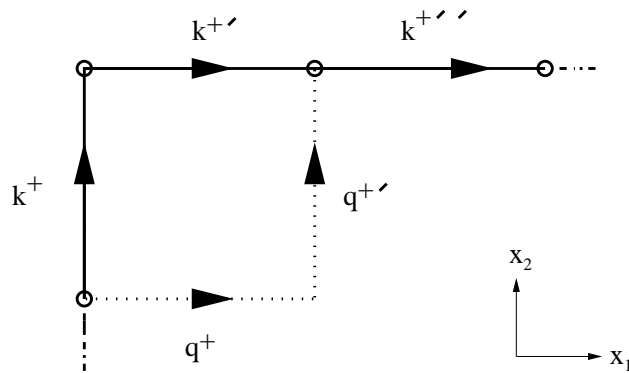


Figure 8: Action of the plaquette operator (79) on successive links in a state. The dotted line represents the final configuration.

Let us illustrate how the dimensional reduction of the Hamiltonian is justified with an example involving the plaquette interaction in Eq.(41)

$$\sum_{r \neq s} \text{Tr} \left\{ M_r(\mathbf{x}) M_s(\mathbf{x} + a\hat{\mathbf{r}}) M_r^\dagger(\mathbf{x} + a\hat{\mathbf{s}}) M_s^\dagger(\mathbf{x}) \right\} . \quad (79)$$

We consider a $2 \rightarrow 2$ amplitude which occurs on neighbouring links in the colour trace of a state (such as Eq.(53)). The operator (79) contains in its mode expansion the combination

$$\text{Tr} \left\{ a_{+1}^\dagger(q^+, \mathbf{x}) a_{+2}^\dagger(q^+, \mathbf{x} + a\hat{\mathbf{1}}) a_{+1}(k^+, \mathbf{x} + a\hat{\mathbf{2}}) a_{+2}(k^+, \mathbf{x}) \right\} , \quad q^+ + q^+ = k^+ + k^+ . \quad (80)$$

Acting upon the successive links illustrated in Fig. 8

$$\text{Tr} \left\{ \cdots a_{+2,kj}^\dagger(k^+, \mathbf{x}) a_{+1,ji}^\dagger(k^+, \mathbf{x} + a\hat{\mathbf{2}}) a_{+1,ih}^\dagger(k^+, \mathbf{x} + a\hat{\mathbf{2}} + a\hat{\mathbf{1}}) \cdots \right\} |0\rangle \quad (81)$$

the result is to move the first two links diagonally and redistribute the light-cone momentum, yielding

$$N \text{Tr} \left\{ \cdots a_{+1,kj}^\dagger(q^+, \mathbf{x}) a_{+2,ji}^\dagger(q^+, \mathbf{x} + a\hat{\mathbf{1}}) a_{+1,ih}^\dagger(k^+, \mathbf{x} + a\hat{\mathbf{2}} + a\hat{\mathbf{1}}) \cdots \right\} |0\rangle \quad (82)$$

In the dimensionally reduced theory the \mathbf{x} label is dropped. The result this time has an extra term if $k^+ = k^+$ since the second and third links are identified. The extra term is

$$\text{Tr} \left\{ a_{+1}^\dagger(k^+) a_{+1}^\dagger(q^+) a_{+2}^\dagger(q^+) \right\} \text{Tr} \left\{ \cdots \delta_{kh} \cdots \right\} |0\rangle , \quad (83)$$

which is suppressed by $1/N$ compared to (82). In fact, the first colour trace in (83) represents a winding mode around the compactified lattice (see (77)). Note that, aside from momentum conservation, the longitudinal coordinate plays no role in the calculation; it is only the colour index structure that is important. The generalisation of these arguments to other gauge invariant operators in the Hamiltonian that contain a finite number number of link fields is straightforward, showing that additional interactions that appear due to compactification are suppressed in the $N \rightarrow \infty$ limit. The Hamiltonian in the basis of reduced states may also be evaluated at non-zero \mathbf{P} , by boosting with the M^{+r} generator without loss of generality [31].

Note that the Eguchi-Kawai reduction is exact, provided that $|0\rangle$ is the true vacuum. This is only the true vacuum in the colour-dielectric regime, which does not contain the transverse continuum limit. This is consistent with the finding in other lattice quantization schemes, where the naive reduction is only valid on coarse lattices [38].

3 A solution of pure gauge theory at large N

In this section, we outline an explicit solution of a transverse lattice gauge theory [39, 40]. It aims to produce results for the low-lying glueball boundstates of QCD to leading order in the $1/N$ expansion. This will be achieved by renormalising couplings (non-perturbatively) so as to approximately restore continuum symmetries violated by the lattice cut-off. QCD may be *defined* as that local quantum field theory with gauge, Poincaré, chiral, parity, and charge conjugation symmetries that has the asymptotically free continuum limit. We will make the additional, but reasonable, assumption of universality. That is, the continuum limit of QCD is unique in the sense that it cannot be continuously deformed

into another theory, with the same definition, that gives different answers. In other words, there are no adjustable dimensionless parameters in QCD, although a dimensionful confinement scale, such as $\sqrt{\sigma}$, must be taken from experiment. (We regard the quark masses as part of the electroweak action). If P^- is the light-cone Hamiltonian of QCD without approximation, its eigenvalues should take the relativistic form

$$P^- = \frac{\mathcal{M}^2 + |\mathbf{P}|^2}{2P^+}, \quad (84)$$

for eigenstates of momentum P^+ and \mathbf{P} .

Once a cut-off is introduced, some of the symmetries of QCD will be broken. For generality, we must now include in the action couplings to terms that preserve only the residual symmetries unviolated by the cut-off. Thus, on a transverse lattice we should include couplings that preserve only gauge symmetry, 90°-rotations about x^3 , boosts along x^3 , etc. In general, there are an infinite number of possible terms one could add. The idea behind renormalisation of Hamiltonians is that, as the cut-off varies, these extra couplings can be tuned so as to maintain the same eigenvalues of P^- , at least for the accessible momenta in the presence of the cut-off.³ The extra couplings which are allowed, once one breaks continuum symmetries, are thus not independent. In particular there should be a particular region of coupling space, over which the cut-off varies, which gives the same eigenvalues for P^- as the continuum limit.

In the previous section we developed a transverse lattice gauge theory with linear link variables M quantized about the $M = 0$ vacuum — the colour-dielectric regime. There is always a cut-off in this theory, since the transverse continuum limit cannot be directly accessed without dealing with a new vacuum problem. Treating this as an effective theory, one would normally expect to be able to tune some of the couplings to restore symmetry and have to fix the remaining ones phenomenologically (they would ultimately be determined by the fundamental physics above the momentum cut-off). However, at least in the case of pure gauge theories, evidence has been found that symmetry constraints alone can accurately determine couplings on the transverse lattice. A possible explanation of this is that, on the transverse lattice, one always works in the continuum limit of QCD in the x^0 and x^3 directions, meaning that restoration of full space-time symmetry should pick out QCD and not some other continuum limit of the lattice gauge theory. The requirements of Lorentz covariance and explicit gauge invariance seem to be very restrictive in this formulation. In practice one searches the space of couplings to see if one can reproduce the continuum momentum dependence of eigenvalues Eq. (84). The reasoning is that if we would follow such a symmetry-restoring region all the way to the continuum limit $a = 0$, this would be the continuum limit of QCD if the uniqueness assumptions above are valid. Note that we do not demand anything of the masses \mathcal{M} in Eq. (84), only the relativistic form of dispersion. These masses should remain invariant in the symmetry-restoring region of couplings, if QCD is unique, whatever the cut-off, and represent a prediction of the theory.

In order to explore coupling constant space, one must first introduce an approximation scheme for the cut-off Hamiltonian, to render the number of couplings finite. So it is necessary to introduce criteria for deciding which are the most important for the physics to be studied and how symmetries will be restored approximately. One searches for a finite-dimensional approximation \mathcal{T}_s to a renormalised trajectory \mathcal{T}

³Some of the first attempts to formulate renormalisation group ideas focussed on Hamiltonians [41]. An interesting weak-coupling renormalisation scheme for light-cone Hamiltonians has been developed in ref.[42]. Since it relies heavily upon running couplings in the neighborhood of the continuum limit, so that asymptotic freedom allows the perturbative renormalisation of couplings, it is not suited to the coarse transverse lattice.

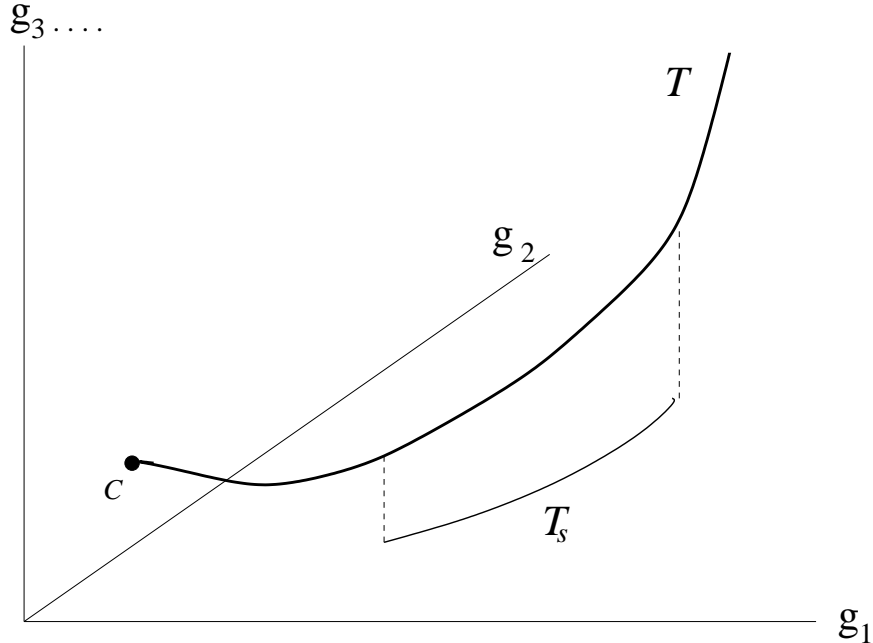


Figure 9: $\{g_1, g_2, g_3, \dots\}$ represents an infinite dimensional space of allowed couplings in the cut-off Hamiltonian, $\{g_1, g_2\}$ a finite-dimensional subspace accessible in practice. \mathcal{T} is the renormalised trajectory that produces the same eigenvalues as continuum QCD Eq. (84), \mathcal{T}_s an approximation to it, \mathcal{C} the intersection of \mathcal{T} with the continuum $a = 0$.

(see Fig. 9).

3.1 Topography of coupling space

A systematic framework for studying the pure glue transverse lattice Hamiltonians was introduced in ref.[22] and developed in refs.[30, 31, 32, 39, 40]. Firstly, if we demand that P^+ remains a kinematic operator (independent of interactions), then the kinetic term for link fields and sources in the continuous directions is restricted to the quadratic forms given in Eq. (40) and Eq. (66). We have much more freedom to choose the potential $U_{\mathbf{x}}(M)$, generalising the form Eq. (41). One idea is to expand the Hamiltonian that results from it in powers of the dynamical link-field M (after elimination of non-dynamical fields A_{\pm}). Such a ‘‘colour-dielectric’’ power expansion can only be justified in a region of coupling space where these fields are sufficiently heavy that light-cone wavefunctions of interest converge quickly in link-field number. For sufficiently heavy fields, the lowest-mass lattice hadrons will consist of a few partons M with little mixing into configurations with many partons. Because of the special properties of light-cone co-ordinates, noted in Sec. 1.1, fields do not have to be very heavy at all for this to be viable. The physical motivation for expecting a renormalised trajectory to exist in the region of link-fields M with positive mass squared is the colour-dielectric picture of confinement [1, 18]. Gauge symmetry, residual Poincaré symmetry, dimensional counting in the continuous directions (x^+, x^-) ,⁴

⁴Operators should be of dimension two or less with respect to scaling of the continuous co-ordinates (x^0, x^3) , as in a 1 + 1 dimensional field theory. In 1 + 1 dimensions, fermions Ψ have dimension 1/2, while link fields behave like scalars, with dimension 0.

together with this power expansion in dynamical fields, limits the number of allowed operators in $U_{\mathbf{x}}(M)$. If we also work to leading order of the $1/N$ expansion, then we can also take advantage of the simplifications noted in section 2.4. In refs.[39, 40] the most general transversely-local pure glue Hamiltonian to order M^4 and most general heavy source Hamiltonian to order M^2 was studied in the large- N limit. The potential that produces it is

$$\begin{aligned}
U_{\mathbf{x}} = & \mu_b^2 \sum_r \text{Tr}\{M_r M_r^\dagger\} - \frac{\beta}{Na^2} \sum_{r \neq s} \text{Tr}\{M_r(\mathbf{x}) M_s(\mathbf{x} + a\hat{\mathbf{r}}) M_r^\dagger(\mathbf{x} + a\hat{\mathbf{s}}) M_s^\dagger(\mathbf{x})\} \\
& + \frac{\lambda_1}{a^2 N} \sum_r \text{Tr}\{M_r M_r^\dagger M_r M_r^\dagger\} + \frac{\lambda_2}{a^2 N} \sum_r \text{Tr}\{M_r(\mathbf{x}) M_r(\mathbf{x} + a\hat{\mathbf{r}}) M_r^\dagger(\mathbf{x} + a\hat{\mathbf{r}}) M_r^\dagger(\mathbf{x})\} \\
& + \frac{\lambda_3}{a^2 N^2} \sum_r \left(\text{Tr}\{M_r M_r^\dagger\}\right)^2 + \frac{\lambda_4}{a^2 N} \sum_{\sigma=\pm 2, \sigma'=\pm 1} \text{Tr}\{M_\sigma^\dagger M_\sigma M_{\sigma'}^\dagger M_{\sigma'}\} \\
& + \frac{4\lambda_5}{a^2 N^2} \text{Tr}\{M_1 M_1^\dagger\} \text{Tr}\{M_2 M_2^\dagger\} \\
& - \frac{\tau_1}{NG^2} \sum_r \text{Tr}\{F^{\alpha\beta} F_{\alpha\beta} (M_r^\dagger M_r + M_r M_r^\dagger)\} \\
& - \frac{\tau_2}{NG^2} \sum_r \text{Tr}\{M_r^\dagger(\mathbf{x}) F^{\alpha\beta}(\mathbf{x}) M_r(\mathbf{x}) F_{\alpha\beta}(\mathbf{x} + a\hat{\mathbf{r}})\} . \tag{85}
\end{aligned}$$

We have defined $M_r = M_{-r}^\dagger$ and hold $\overline{G} \rightarrow G\sqrt{N}$ finite in the $N \rightarrow \infty$ limit, using it to set the single dimensionful scale of pure gauge theory. Dimensionless versions of the other couplings can then be constructed

$$m_b^2 = \frac{\mu_R^2}{\overline{G}^2}, \quad l_i = \frac{\lambda_i}{a^2 \overline{G}^2}, \quad t_i = \frac{\tau_i}{\overline{G}}, \quad b = \frac{\beta}{a^2 \overline{G}^2}. \tag{86}$$

Note that the dimensionless mass m_b is made from the renormalised mass μ_R (see Eq.(52)). One parameter should play the role of a dimensionless lattice spacing, $a\overline{G}$. This space of couplings Eq. (86) was searched and the eigenvalues of P^- found for various momenta. A χ^2 -test of symmetry restoration, including variables to quantify deviation from relativistic dispersion Eq. (84) in low-mass glueballs and rotational invariance of the heavy source potential, produced a ‘topography’ of coupling space partly illustrated in Fig. 10. For each pair of couplings, all other couplings were varied.

The bottom of the valley in each of these diagrams represents (a projection of) \mathcal{T}_s , the best approximation to a renormalised trajectory. There are a number of reasons to believe that this feature is not accidental: it appears in every figure, no matter how you slice the space; it is robust under changes of the χ^2 test; each valley has a flat direction (parameterized by $a\overline{G}$); low-lying invariant masses \mathcal{M} scale approximately along the valley and agree with large- N extrapolations of glueballs masses computed by quenched finite- N Euclidean lattice methods, that do not make a colour-dielectric expansion [43].⁵ The glueball spectrum has also been estimated [44] for $SU(3)$ using the light-cone methods of refs.[42], and in the large- N limit using a conjectured relation to supergravity [45].

Most importantly, the light-cone wavefunctions are found to be concentrated on particular numbers of links, meaning that the expansion of the Hamiltonian in link-fields is self-consistent. In the region of

⁵Similar results have been produced for pure gauge theory in 2 + 1-dimensions [31, 46, 47], where greater precision is possible.

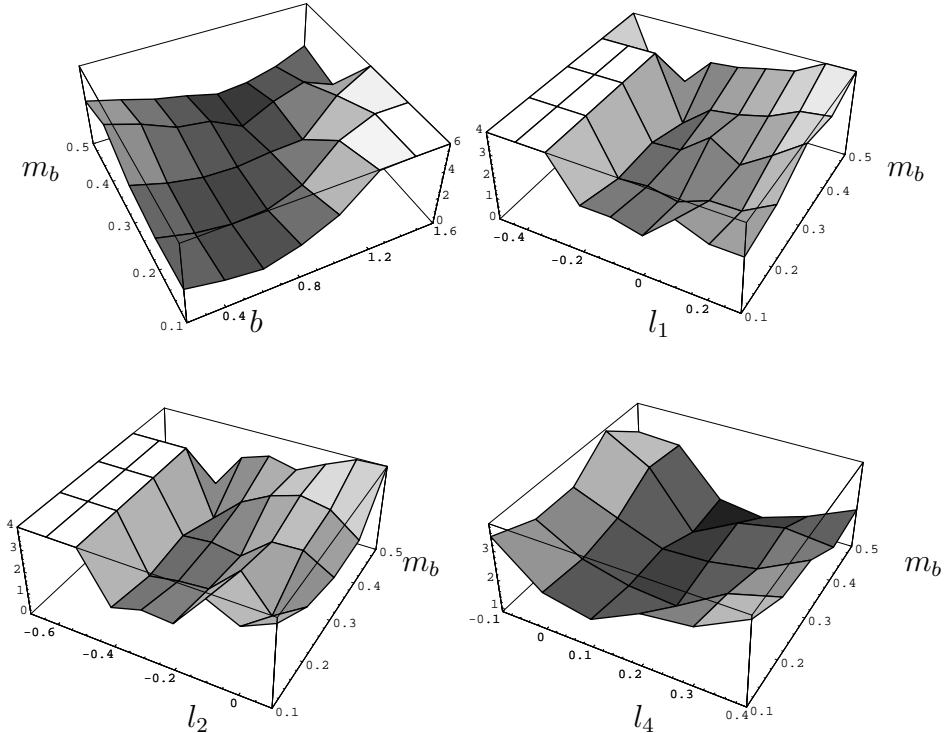


Figure 10: Charts of coupling space with a χ^2 -test of symmetry restoration.

\mathcal{T}_s that is accessible in the colour-dielectric regime, the lattice spacing a is of order 0.65 fm and varies only by about 10%. If the discretization is made too coarse, tuning the couplings in $U_x(M)$ Eq. (85) is insufficient to produce a clear valley. If a is made too small, the link mass m_b becomes tachyonic, requiring quantization about a new vacuum. It is not yet known whether the above analysis again picks out an unambiguous trajectory at higher orders of the colour-dielectric expansion.

3.2 Results for glueball boundstates

In this section we extract some possible lessons for glueball phenomenology from large- N calculations on the transverse lattice. Quantitative comparison with experimental results in this sector will require the computation of corrections to the large- N limit, so as to take account of mixing and decay into mesons.

Because there are no quark loops in the large- N limit, the transverse lattice result for glueballs should equal the large- N limit of full QCD, not only its quenched approximation. Fig. 11 illustrates, moreover, how remarkably close the large- N limit is to even $N = 2$ pure glue, so far as low-lying masses are concerned. A priori there is no reason to expect this. For those glueballs where the OZI rule is valid, QCD itself should yield answers close to that of the large- N limit. If the large- N limit is a good approximation to QCD, this implies that glueballs can be accurately pictured as a single connected loop of flux. This is the basis of string [49, 50] and flux-tube models [51, 52] of glueball dynamics. These models also predict an exponentially rising density of states, which also occurs in the transverse lattice spectrum [31], and is ultimately responsible for the finite temperature phase transition of pure gauge

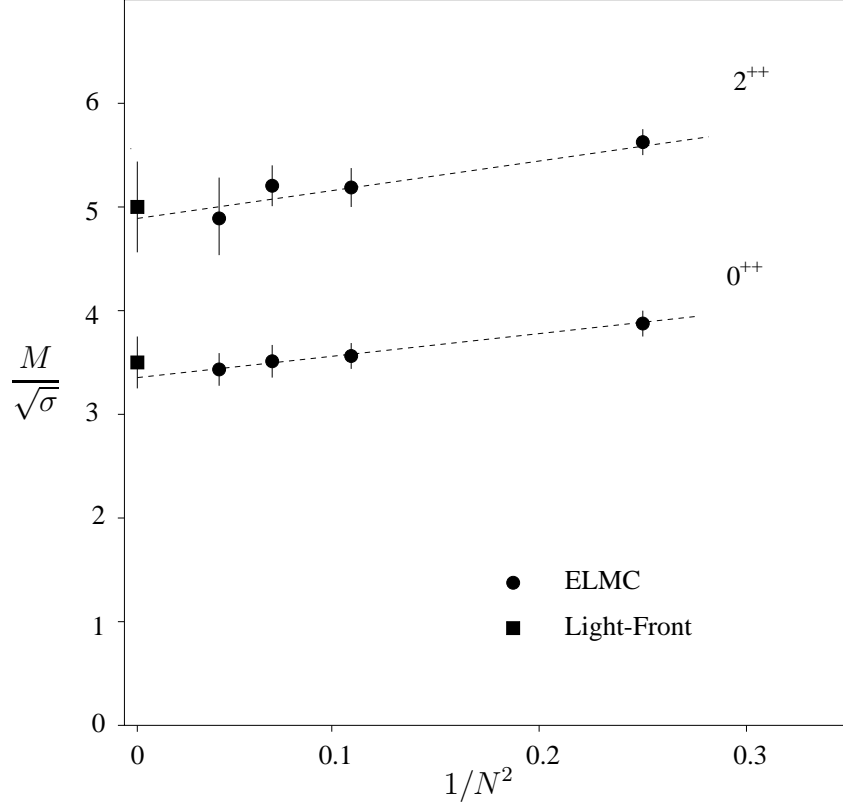


Figure 11: The variation of glueball masses with N (pure glue). The transverse lattice results [40] for scalar and tensor glueballs are denoted by boxes. Euclidean Lattice Monte Carlo (ELMC) predictions are given by circles and compiled for $N = 2, 3, 4, 5$ [48, 43]. The chain lines are a fit to the form $A + B/N^2$ based on finite- N data [43].

theory [53].

What about the structure on this single loop? In the transverse plane, about 90% of the wavefunction in low-lying glueballs is concentrated in an area of order one lattice spacing across. Even with such a coarse cut-off, any amount of structure can be accommodated because, unlike unitary matrix link variables, complex links can back-track any number of times. Fig. 12 shows the distribution of P^+ longitudinal momentum fraction x among the link partons in the lightest large- N glueball:

$$\begin{aligned}
G_d(x, 1/a) &= \frac{1}{2\pi x P^+} \int dx^- e^{-ixP^+x^-} \langle \psi(P^+) | \text{Tr} \{ \partial_- M_r \partial_- M_r^\dagger \} | \psi(P^+) \rangle \\
&= \langle \psi(P^+) | a_{\lambda,ij}^\dagger(xP^+, \mathbf{x}) a_{\lambda,ij}(xP^+, \mathbf{x}) | \psi(P^+) \rangle .
\end{aligned} \tag{87}$$

G_d is the expectation of the number operator for links of momentum fraction x , exactly satisfies the momentum sum rule

$$\int_0^1 dx x G_d(x) = 1 , \tag{88}$$

and becomes the gluon distribution in the limit $a \rightarrow 0$. At finite a , M is a collective gluon excitation. The momentum sum rule would therefore naïvely predict the gluon distribution to be even softer than G_d , since every link is a superposition of gluons carrying only a fraction of its momentum. In this case,

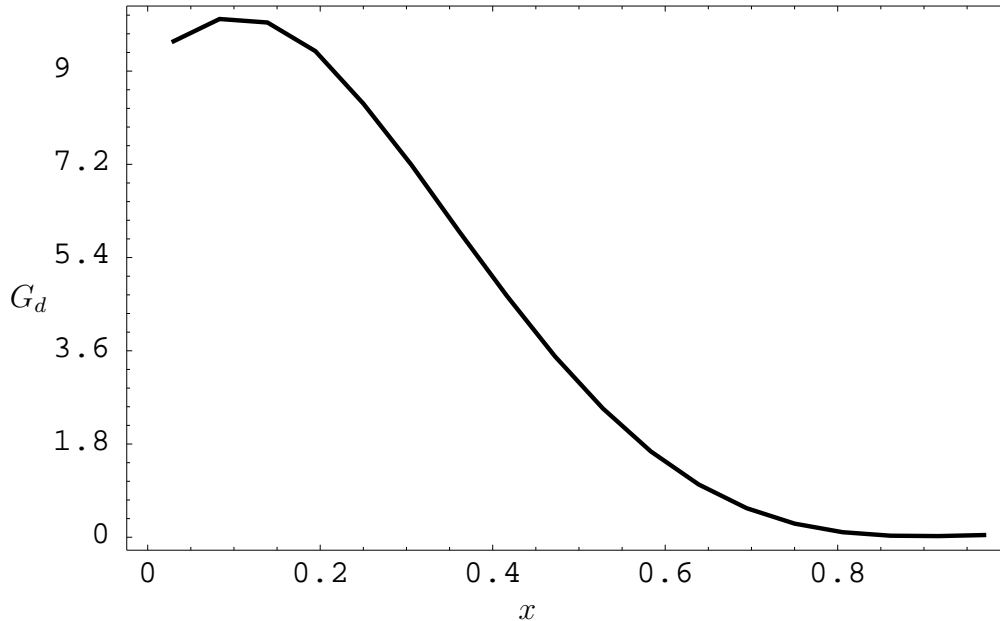


Figure 12: The distribution of P^+ momentum fraction x in the 0^{++} glueball at large N .

the 0^{++} glueball wavefunction seems to have many gluons and does not resemble gluonium (two-gluon boundstate), which would have a distribution symmetric about $x = 0.5$. The relationship between this result and constituent gluon models [54], where the lightest glueball *is* gluonium, is presumably same as that between other hadronic structure functions and the constituent quark model. The latter would have us believe the nucleon is three quarks and the meson two, when in fact only half the momentum is typically carried by quarks in a fully relativistic description. The missing momentum is carried by gluons ‘in flight’ that are the true source of binding modeled by first-quantized potentials. In glueballs, it so happens that the forces and constituents are made of the same stuff. This result implies one should be cautious about using a two-gluon model for glueballs in a relativistic context; for example, when trying to predict branching ratios [55].

4 Mesons on the transverse lattice

In this section we will introduce fermions on the transverse lattice and discuss issues that are specific for fermions in this framework. Some of them, such as species doubling, are familiar from other frameworks, while others, such as the issue of vacuum condensates, seem to be specific to the light-cone formulation. We then go on to construct meson boundstates in gauge theory.

4.1 Formulation of the light-cone Hamiltonian with fermions

The simplest fermion Lagrangian for the transverse lattice, which satisfies gauge invariance and reduces in the naive continuum limit $a \rightarrow 0$ to the continuum QCD action, reads

$$L = a^2 \sum_{\mathbf{x}} \int dx^- \left[\bar{\Psi}(\mathbf{x}) (i\gamma^\alpha D_\alpha - \mu_f) \Psi(\mathbf{x}) + i \sum_s \bar{\Psi}(\mathbf{x}) \gamma^s \frac{M_s(\mathbf{x}) \Psi(\mathbf{x} + a\hat{s}) - M_s^\dagger(\mathbf{x} - a\hat{s}) \Psi(\mathbf{x} - a\hat{s})}{2a} \right], \quad (89)$$

where the fermion fields are defined on the sites of the transverse lattice. Fermion fields map under transverse lattice gauge transformations $U(\mathbf{x}, x^+, x^-) \in SU(N)$ as

$$\Psi(\mathbf{x}) \rightarrow U(\mathbf{x})\Psi(\mathbf{x}) . \quad (90)$$

The naive transverse derivative term in Eq. (89) exhibits the familiar problem of ‘species doubling’, i.e. it yields too many low energy degrees of freedom in the continuum limit. To see this, consider the above transverse derivative for free fields ($M_s \equiv 1$). In this case the Lagrangian becomes

$$L_{\perp} \equiv \sum_{\mathbf{x}} \int dx^- \bar{\Psi}(\mathbf{x}) i\gamma^s \frac{\Psi(\mathbf{x} + a\hat{\mathbf{s}}) - \Psi(\mathbf{x} - a\hat{\mathbf{s}})}{2a} . \quad (91)$$

Note that we have chosen a lattice representation for the transverse derivative that involves a difference between fields on sites that are separated by two lattice spacing $\Psi(\mathbf{x} + a\hat{\mathbf{s}}) - \Psi(\mathbf{x} - a\hat{\mathbf{s}})$ in order to obtain a manifestly Hermitian Lagrangian. Replacing the derivative terms in the action by expressions like Eq. (91) leads to ‘species doubling’ in the sense that multiplying any solution to the free Dirac equation by a rapidly oscillating transverse phase factor yields another solution with the same energy. As a result, low momentum solutions are degenerate with solutions near the edge of the Brillouin zone and therefore too many low energy degrees of freedom remain in the continuum limit. Other, more complicated, discrete representations of the transverse derivatives exhibit similar problems. This is not an accident because the Nielsen-Ninomiya theorem [56] — this states that any local, Hermitian and chirally invariant fermion kinetic term necessarily exhibits species doubling — also applies here. Although the use of the colour-dielectric expansion means that ultimately we will be interested in the transverse lattice theory far from the continuum, the problem that leads to species doubling is still relevant because it entails bad dispersion. The dispersion induced by Eq. (91) at finite lattice spacing is considerably worse than that of a scalar hopping term.

Similar to the situation in Euclidean and equal- x^0 Hamiltonian lattice gauge theories, there exist several options to deal with this situation. Here we will focus on generalizations of Wilson fermions to the transverse lattice.⁶ The role of Wilson fermions on a coarse lattice will be to improve the bad dispersion.

The basic reason for the appearance of doublers in lattice actions for fermions is the fact that the continuum action is first order in the derivative. Therefore, one natural way to remove doublers is to add to the Lagrangian a term

$$L_r = ra^3 \int dx^- \sum_{\mathbf{x}} \sum_s \bar{\Psi}(\mathbf{x}) \frac{M_s(\mathbf{x})\Psi(\mathbf{x} + a\hat{\mathbf{s}}) - 2\Psi(\mathbf{x}) + M_s^\dagger(\mathbf{x} - a\hat{\mathbf{s}})\Psi(\mathbf{x} - \hat{\mathbf{s}})}{a^2} \\ \xrightarrow{\text{continuum}} ar \int dx^- d^2\mathbf{x} \bar{\Psi} D_s^2 \Psi , \quad (92)$$

where $r = \mathcal{O}(1)$ is a dimensionless number. In order to remove doublers both for particles and antiparticles, the added term has the Dirac structure of a mass term, which breaks chiral symmetry explicitly.

After adding such a Wilson term to the Lagrangian fermions on the transverse lattice, one can proceed with canonical light-cone quantization. Firstly, one eliminates the constrained fermion component

⁶Staggered fermions have been investigated on the transverse lattice in Refs. [1, 57].

$\Psi_{(-)} \equiv \frac{\gamma^- \gamma^+}{2} \Psi$ using the classical equations of motion. In the next step, one rescales the dynamical component $\Psi_{(+)} \equiv \frac{\gamma^+ \gamma^-}{2} \Psi$ such that there are no dimensionful couplings multiplying the x^+ derivative term, i.e. we introduce

$$\Phi(\mathbf{x}) \equiv a \Psi_{(+)}(\mathbf{x}) , \quad (93)$$

in terms of which the term containing a light-cone time derivative has the form of a 1 + 1 dimensional field theory at each lattice site

$$L_{kin} \equiv a^2 \int dx^- \sum_{\mathbf{x}} i \bar{\Psi}(\mathbf{x}) \gamma^+ \partial_+ \Psi(\mathbf{x}) = \int dx^- \sum_{\mathbf{x}} i \bar{\Phi}(\mathbf{x}) \gamma^+ \partial_+ \Phi(\mathbf{x}) . \quad (94)$$

It is convenient to use a chiral representation, where $\bar{\Psi}^\dagger = (u_+^*, v_+^*, v_-^*, u_-^*)/a2^{1/4}$ decomposes into left (right) movers v (u) with sign of helicity $h = \pm$. The symbol $*$ means complex conjugate, and from now on we assume the transposition in hermitian conjugate \dagger acts on colour indices. In terms of these one finds

$$L_{kin} = \int dx^- \sum_{\mathbf{x}} \sum_{h=\pm} u_h^\dagger(\mathbf{x}) \gamma^+ \partial_+ u_h(\mathbf{x}) , \quad (95)$$

and therefore the canonical anti-commutation relations at equal light-cone times x^+ are

$$\begin{aligned} \{u_h(\mathbf{x}), u_{h'}^*(\mathbf{y})\} &= \delta_{hh'} \delta_{\mathbf{xy}} \delta(x^- - y^-) \\ \{u_h(\mathbf{x}), u_{h'}(\mathbf{y})\} &= \{u_h^*(\mathbf{x}), u_{h'}^*(\mathbf{y})\} = 0 . \end{aligned} \quad (96)$$

For the Fock expansion we employ again a convenient mixed representation, using longitudinal (continuous) momentum and transverse (discrete) position variables

$$u_h(x^+ = 0, x^-, \mathbf{x}) = \frac{1}{\sqrt{2\pi}} \int_0^\infty dk^+ [b_h(k^+, \mathbf{x}) e^{-ik^+ x^-} + d_{-h}^*(k^+, \mathbf{x}) e^{ik^+ x^-}] \quad (97)$$

with

$$\begin{aligned} \{b_h(k^+, \mathbf{x}), b_{h'}^*(\tilde{k}^+, \mathbf{y})\} &= \delta_{hh'} \delta_{xy} \delta(k^+ - \tilde{k}^+) \\ \{b_h(k^+, \mathbf{x}), b_{h'}(\tilde{k}^+, \mathbf{y})\} &= \{b_h^*(k^+, \mathbf{x}), b_{h'}^*(\tilde{k}^+, \mathbf{y})\} = 0 , \end{aligned} \quad (98)$$

and likewise for $d_h^*(k^+, \mathbf{x})$. $b_h^*(k^+, \mathbf{x})$ and $d_h^*(k^+, \mathbf{x})$ have the usual interpretation as creation operators for a quark/antiquark with momentum k^+ and sign of helicity $h \in \{\pm\}$ on the transverse site \mathbf{x} .

If we order the terms in the Hamiltonian $P^- = a^2 \sum_x \int dx^- \mathcal{H}$ according to the powers of the interactions, to second order in the fields we find a ‘kinetic energy’ term

$$\mathcal{H}^{(2)}(\mathbf{x}) = \left(\mu_f + \frac{2r}{a} \right)^2 \bar{\Phi}(\mathbf{x}) \frac{1}{i\sqrt{2}\partial_-} \Phi(\mathbf{x}) . \quad (99)$$

To third order, we obtain both a local ‘1 + 1 Coulomb’ term as well as a transverse hopping term

$$\mathcal{H}^{(3)}(\mathbf{x}) = \mathcal{H}_{Coul.}^{(3)}(\mathbf{x}) + \mathcal{H}_{hopp.}^{(3)}(\mathbf{x}) . \quad (100)$$

The Coulomb coupling for fermions is local in the transverse direction because both the fermions as well as the longitudinal gauge field A_+ are defined on the sites of the transverse lattice

$$\mathcal{H}_{Coul.}^{(3)}(\mathbf{x}) = \frac{G}{\sqrt{N}} \Phi^\dagger(\mathbf{x}) \gamma^+ A_+(\mathbf{x}) \Phi(\mathbf{x}) . \quad (101)$$

One obtains both transverse hopping terms that flip the helicity of the fermions as well as terms that do not flip the helicity

$$\mathcal{H}_{hopp}^{(3)}(\mathbf{x}) = \kappa_a \mathcal{H}_{flip}^{(3)}(\mathbf{x}) + \kappa_s \mathcal{H}_{noflip}^{(3)}(\mathbf{x}) , \quad (102)$$

where

$$\mathcal{H}_{flip}^{(3)}(\mathbf{x}) = i \sum_r \Phi^\dagger(\mathbf{x}) \frac{\gamma^r}{i\partial_-} \left[M_r(\mathbf{x}) \Phi(\mathbf{x} + a\hat{r}) - M_r^\dagger(\mathbf{x} - a\hat{r}) \Phi(\mathbf{x} - a\hat{r}) \right] , \quad (103)$$

and

$$\mathcal{H}_{noflip}^{(3)}(\mathbf{x}) = \sum_r \Phi^\dagger(\mathbf{x}) \frac{1}{i\partial_-} \left[M_r(\mathbf{x}) \Phi(\mathbf{x} + a\hat{r}) + M_r^\dagger(\mathbf{x} - a\hat{r}) \Phi(\mathbf{x} - a\hat{r}) \right] . \quad (104)$$

The relation between the bare couplings and the coefficients of the hopping terms is given by

$$\begin{aligned} \kappa_a &= -\frac{\mu_f + \frac{2r}{a}}{2\sqrt{2}a} \\ \kappa_s &= -r \frac{\mu_f + \frac{2r}{a}}{\sqrt{2}a} . \end{aligned} \quad (105)$$

We should emphasize that these hopping terms also represent the most general terms bilinear in fermions and linear in the link fields which are invariant under those symmetries that are not broken by the transverse lattice. Therefore, even though we have used canonical reasoning to derive these terms, they also appear naturally in the colour dielectric expansion at third order in the fields.

An interesting feature of the light-cone formulation is that the fermion kinetic energy is quadratic in the transverse derivative after eliminating the constrained component of the fermion field. For free fields in the continuum

$$\mathcal{H}_{kin} = \Phi^\dagger(\mathbf{x}) \frac{\mu_f^2 - \partial_r^2}{i\sqrt{2}\partial_-} \Phi(\mathbf{x}) . \quad (106)$$

Therefore, if one discretizes the free field transverse lattice Hamiltonian *after* eliminating $\Psi_{(-)}$, it appears possible to write down a discretized Hamiltonian for fermions which does not exhibit species doubling [58]

$$\mathcal{H}_{kin}^{latt} \sim \Phi^\dagger(\mathbf{x}) \frac{\mu_f^2}{i\sqrt{2}\partial_-} \Phi(\mathbf{x}) - \sum_r \Phi(\mathbf{x}) \frac{1}{i\sqrt{2}\partial_-} \frac{\Phi(\mathbf{x} + a\hat{r}) - 2\Phi(\mathbf{x}) + \Phi(\mathbf{x} - a\hat{r})}{a^2} . \quad (107)$$

In fact, in the light-cone formulation of the transverse lattice there appears to be a whole class of light-cone Hamiltonians that do not exhibit species doubling and yet they are chirally invariant when $\mu_f = 0$. To see this, let us introduce a modified r -term [58]

$$\begin{aligned} \tilde{L}_r &= a\tilde{r} \int d^2\mathbf{x} \int dx^- \sum_s \bar{\Psi} \frac{\gamma^+}{2i\partial_-} D_s^2 \Psi \\ &\xrightarrow{lattice} a\tilde{r} \sum_{\mathbf{x}} \int dx^- \sum_s \bar{\Psi}(\mathbf{x}) \frac{\gamma^+}{2i\partial_-} \left[M_s(\mathbf{x}) \Psi(\mathbf{x} + a\hat{s}) - 2\Psi(\mathbf{x}) + M_s^\dagger(\mathbf{x} - a\hat{s}) \Psi(\mathbf{x} - a\hat{s}) \right] . \end{aligned} \quad (108)$$

Note that \tilde{r} has dimensions of mass because of the extra $1/\partial_-$. This modified r -term is chirally invariant because of the γ^+ matrix in between the bilinear $\bar{\Psi}\Psi$. It is Hermitian as well as local in the transverse direction. However, it is non-local in the x^- direction, but the non-locality is of the same type $\sim \frac{1}{i\partial_-}$ as many other terms that one has to deal with in the light-cone formulation, and therefore one should consider this as a possible alternative to the standard Wilson approach.

If one repeats the light-cone Hamiltonian quantization with such a modified r term, one obtains the same hopping terms as in the usual Wilson approach Eqs. (103, 104). It should not be surprising that these operators appear also here since they represent the most general hopping terms that are permitted by symmetry to this order. However, what does change is the dependence of the coefficients of these terms on μ_f and \tilde{r} . One finds [58]

$$\begin{aligned}\kappa_a &= -\frac{\mu_f}{2\sqrt{2}a} \\ \kappa_s &= -\frac{\tilde{r}}{2\sqrt{2}a}.\end{aligned}\tag{109}$$

Eq. (109) also shows explicitly that, even in the presence of the (modified) r term, fermion helicity is conserved for $\mu_f \rightarrow 0$. This reflects the fact that fermion helicity is conserved in the chiral limit of QCD . These issues are discussed in further detail in the appendix.

4.2 Numerical studies of light mesons

We now apply the ideas to the practical calculation of light meson boundstates. The Hamiltonians we have discussed so far for fermions on the transverse lattice contain the following parameters (in addition to pure glue parameters)

1. A (kinetic) mass term for the fermions. In numerical calculations that employ a truncation of the Fock expansion, it is in general necessary to make this mass term Fock sector dependent. For example, if one truncates the Fock expansion above three particles (q , \bar{q} , plus at most one link quantum) then the mass of fermions in the two particle Fock component gets renormalised due to the ‘dressing’ of fermions with one link quantum. However, the truncation of Fock space would not permit the same dressing for a fermion that is already in the three particle Fock component — a process that is also generated by the Hamiltonian if no Fock space truncation is used. In order to compensate for this effect, it is necessary to allow for Fock sector dependent masses in the Hamiltonian.⁷
2. The helicity flip and noflip couplings κ_a and κ_s
3. The coupling G of fermions to the longitudinal component of the gauge field A_+ . This coupling constant is the same for fermions and link fields because of gauge invariance.

We should also comment here on the issue of dynamical (spontaneous) chiral symmetry breaking. In the light-cone formulation, physical states are constructed by applying creation operators to the Fock vacuum. The Fock vacuum is an eigenstate of the light-cone Hamiltonian, which at first appears to exclude any possibility for a complex vacuum structure and spontaneous symmetry breaking phenomena. However, first of all the trivial Fock vacuum does not contradict nonzero vacuum condensates. In fact, recently it has been demonstrated that nontrivial vacuum condensates are obtained within the light-cone framework, if the operator products appearing in those condensates are defined through a point-splitting procedure [60]. Many model studies over the last years have demonstrated that nontrivial

⁷We should also emphasize that these kinds of issues also arise if the only cutoff used is a DLCQ cutoff — even if no Fock space truncation or any other truncation is applied. In this case one would need to allow for a momentum dependent mass in the Hamiltonian [59].

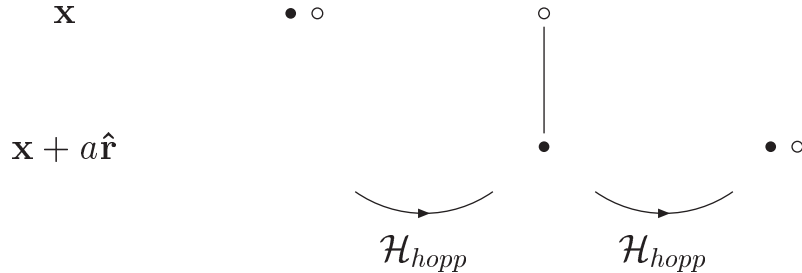


Figure 13: From left to right: sequence of ‘hopping’ interactions that leads to transverse propagation (‘hopping’) of meson by one lattice unit from site \mathbf{x} to site $\mathbf{x} + a\hat{\mathbf{r}}$. The black and open dot represent the quark and antiquark respectively.

vacuum structure does not disappear on the light-cone, but is rather shifted from the states to the operators. Therefore, on the transverse lattice one expects that the coefficients of operators in the Hamiltonian are renormalised in a non-trivial way due to such “vacuum effects”.

The first study of meson spectra and structure on the transverse lattice was done in Ref. [58], where one can also find a more detailed discussion of species doubling within this framework. In that work, the form that we described above was chosen for the Hamiltonian. The numerical work in Ref. [58] employed a ‘femtoworm approximation’, where the meson Fock space is truncated above three particles (i.e. at most one link quantum in addition to the $q\bar{q}$ pair). This is the smallest Fock space that allows transverse propagation of mesons and hence a dependence of the energy P^- on \mathbf{P} . Transverse propagation proceeds by hopping of a quark (or antiquark) by one link, which implies creation of a link quantum on the link connecting the $q\bar{q}$ pair. The antiquark (quark) then follows, absorbing the link quantum in the process (Fig. 13). Transverse propagation over several links proceeds by repeating the above sequence, which resembles the stretching/contracting motion of an inchworm (on a 1 fermi scale) — hence the name.

The Hamiltonian that was introduced in Ref. [58] was later revisited in Refs. [61, 62]. As a major improvement over Ref. [58], Lorentz invariant π and ρ dispersion relations were required as renormalisation conditions — analogously to the pure glue studies described in Section 2.1. Furthermore, physical transverse lattice spacings, as determined from the meson dispersion relations, were required to agree with the lattice spacings obtained in the pure glue sector ($a \sim \frac{2}{3}$ fm). Finally, the mass splitting within the ρ multiplet, which is another measure for the degree of rotational symmetry breaking, was also considered.

In general, the Fock space for mesons in the large N limit on the transverse lattice consists of open strings of link fields with quarks and antiquarks at the ends. If one truncates the Fock space at two particles then mesons are described as bound states of a quark and an anti-quark on the same site. Since transverse propagation is not possible within this approximation, different transverse sites completely decouple from each other and on each transverse site one obtains the bound state equation and spectrum that are identical to the ones found in large N QCD in 1+1 dimensions [33] where one finds a discrete spectrum of meson states.

The numerical calculations that have been performed so far go one step beyond this lowest order approximation. They are performed in a Fock space that was truncated above three particles (two quarks and one link). For states with vanishing transverse momentum \mathbf{P} , the wavefunction can be written

$$\begin{aligned}
|\psi(P^+)\rangle &= \frac{2a\sqrt{\pi}}{\sqrt{N}} \sum_{\mathbf{x}} \sum_{h,h'} \int_0^{P^+} dk^+ \left\{ \psi_{hh'}(x, 1-x) b_h^\dagger(k^+, \mathbf{x}) d_{h'}^\dagger(P^+ - k^+, \mathbf{x}) |0\rangle \right\} \\
&+ \frac{2a\sqrt{\pi}}{N} \sum_{\mathbf{x}} \sum_{h,h',r} \int_0^{P^+} \frac{dk_1^+ dk_2^+}{P^+} \\
&\times \left\{ \psi_{h(r)h'}(x_1, x_2, 1-x_1-x_2) b_h^\dagger(k_1^+, \mathbf{x}) a_r^\dagger(k_2^+, \mathbf{x}) d_{h'}^*(P^+ - k_1^+ - k_2^+, \mathbf{x} + a\hat{\mathbf{r}}) |0\rangle \right. \\
&\left. + \psi_{h(-r)h'}(x_1, x_2, 1-x_1-x_2) b_h^\dagger(k_1^+, \mathbf{x} + a\hat{\mathbf{r}}) a_{-r}^\dagger(k_2^+, \mathbf{x}) d_{h'}^*(P^+ - k_1^+ - k_2^+, \mathbf{x}) |0\rangle \right\} .
\end{aligned} \tag{110}$$

In this expression \dagger acts on gauge indices and $x = k^+/P^+$ etc.. This truncated expansion for the states simplifies the calculations considerably, but as a result one should not expect restoration of Lorentz symmetry to be as good as in the pure glue calculations of Section 3, where no truncation was made.

For the wavefunction at nonzero transverse momentum $|\psi(P^+, \mathbf{P})\rangle$, an expansion very similar to the one above is made. The only difference is that each term in the summation over transverse lattice sites \mathbf{x} is multiplied by an appropriate phase factor. In Ref. [62] the phase factor chosen for each term was $e^{i\mathbf{x}\cdot\mathbf{P}}$ in the two particle sector, while the terms in the three particle Fock sector were multiplied by a phase $e^{i(\mathbf{x} + \frac{a}{2}\hat{\mathbf{r}})\cdot\mathbf{P}}$, i.e. each state was assigned an effective transverse mean location equal to the midpoint between the quark and the antiquark. In Ref. [61], a slightly different phase convention was made in the 3 particle Fock component; namely, for a state with the quark located on site \mathbf{x} and the antiquark on site $\mathbf{x} + a\hat{\mathbf{r}}$ a phase factor $e^{i\bar{\mathbf{x}}\cdot\mathbf{P}}$ was chosen, where $\bar{\mathbf{x}} = x_1\mathbf{x} + x_3(\mathbf{x} + a\hat{\mathbf{r}}) + (1-x_1-x_3)(\mathbf{x} + \frac{a}{2}\hat{\mathbf{r}})$. The latter choice is physically motivated by use of the transverse boost-rotation operators M_{-r} (c.f. Eqn. (63)), but we should emphasize that both choices are equivalent. The only difference is in the phase convention for the Fock space amplitude of extended states. As long as one uses either choice consistently for the evaluation of physical observables, the phase difference drops out. The wavefunction is normalised covariantly

$$\langle \psi(P_1^+, \mathbf{P}_1) | \psi(P_2^+, \mathbf{P}_2) \rangle = 2P_1^+ (2\pi)^3 \delta(P_1^+ - P_2^+) \delta(\mathbf{P}_1 - \mathbf{P}_2) \tag{111}$$

if

$$1 = \int_0^1 dx \sum_{h,h'} |\psi_{hh'}(x, 1-x)|^2 + \int_0^1 dx_1 dx_2 \sum_{h,\lambda,h'} |\psi_{h(\lambda)h'}(x_1, x_2, 1-x_1-x_2)|^2 . \tag{112}$$

In QCD, dimensionful parameters are the quark masses and the string tension. The string tension is implicitly used if one inputs from the pure glue calculation the numerical value of the longitudinal gauge coupling \tilde{G} as well as the transverse lattice spacing in physical units. The π meson mass can be used to fix the quark masses. In field theory, the mass of the π is related to spontaneous chiral symmetry breaking. A massless pion, in a Lorentz covariant theory, usually means chiral symmetry (realised in the Goldstone mode). The mass *difference* between the π and ρ mesons is also directly related to chiral symmetry breaking in light-cone formalism. One would hope that this scale was generated dynamically once Lorentz covariance is imposed, holding the pion mass at (or near) zero. That is, helicity-violating interactions in the coarse transverse lattice Hamiltonian should be forced to have non-zero couplings,

at least in a truncated Fock space, in order to obtain covariance and a massless pion.⁸ Unfortunately, Lorentz symmetry is sufficiently badly violated in the one-link approximation that this is difficult to verify practice. Other problems of this approximation in implementing this reasoning are that only a single helicity violating interaction $\mathcal{H}_{flip}^{(3)}$ is available and stability of the groundstate is difficult to assess because of the truncation of many-particle states. Calculations so far have therefore modelled the chiral symmetry breaking aspects by fixing the π - ρ mass difference, and hence the helicity violating coupling to $\mathcal{H}_{flip}^{(3)}$ from experiment. A more fundamental understanding of the origin of this term must await relaxation of the one-link approximation.

Using the dimensionful scale $\bar{G} = G\sqrt{(N^2 - 1)/N}$ we introduce the following renormalised dimensionless parameters

$$\frac{\mu_b}{\bar{G}} \rightarrow m_b \ ; \ \frac{\mu_f}{\bar{G}} \rightarrow m_f \ ; \ \frac{\kappa_a\sqrt{2N}}{\mu_f\bar{G}} \rightarrow k_a \ ; \ \frac{\kappa_s\sqrt{2N}}{\mu_f\bar{G}} \rightarrow k_s \ . \quad (113)$$

Using the truncated Fock expansion, we can project the eigenvalue equation $2P^+P^-\psi(P^+) = \mathcal{M}^2\psi(P^+)$ for $\mathbf{P} = 0$ onto Fock basis states, to derive the following set of coupled integral equations for individual Fock amplitudes:

$$\begin{aligned} \frac{\mathcal{M}^2}{\bar{G}^2}\psi_{hh'}(x_1, x_2) &= \left(\frac{m_f^2}{x_1} + \frac{m_f^2}{x_2} \right) \psi_{hh'}(x_1, x_2) + K(\psi_{hh'}(x_1, x_2)) \\ &+ \frac{(k_a^2 + k_s^2)}{\pi} \left(\frac{1}{x_1} \int_0^{x_1} \frac{dy}{y} + \frac{1}{x_2} \int_0^{x_2} \frac{dy}{y} \right) \psi_{hh'}(x_1, x_2) \\ &- \sum_{\lambda} \left\{ \frac{m_f k_s}{2\sqrt{\pi}} \int_0^{x_1} \frac{dy}{\sqrt{y}} \left(\frac{1}{x_1 - y} + \frac{1}{x_1} \right) \psi_{h(\lambda)h'}(x_1 - y, y, x_2) \right. \\ &+ \frac{m_f k_s}{2\sqrt{\pi}} \int_0^{x_2} \frac{dy}{\sqrt{y}} \left(\frac{1}{x_2 - y} + \frac{1}{x_2} \right) \psi_{h(\lambda)h'}(x_1, y, x_2 - y) \\ &+ \frac{\text{Sgn}(\lambda)m_f k_a (hi\delta_{|\lambda|1} + \delta_{|\lambda|2})}{2\sqrt{\pi}} \int_0^{x_1} \frac{dy}{\sqrt{y}} \left(\frac{1}{x_1 - y} - \frac{1}{x_1} \right) \psi_{-h(\lambda)h'}(x_1 - y, y, x_2) \\ &\left. - \frac{\text{Sgn}(\lambda)m_f k_a (h'i\delta_{|\lambda|1} + \delta_{|\lambda|2})}{2\sqrt{\pi}} \int_0^{x_2} \frac{dy}{\sqrt{y}} \left(\frac{1}{x_2 - y} - \frac{1}{x_2} \right) \psi_{h(\lambda)-h'}(x_1, y, x_2 - y) \right\} \ , \end{aligned} \quad (114)$$

$$\begin{aligned} \frac{\mathcal{M}^2}{\bar{G}^2}\psi_{h(\lambda)h'}(x_1, x_2, x_3) &= \left(\frac{m_b^2}{x_2} + \frac{m_f^2}{x_1} + \frac{m_f^2}{x_3} \right) \psi_{h(\lambda)h'}(x_1, x_2, x_3) + K(\psi_{h(\lambda)h'}(x_1, x_2, x_3)) \\ &- \frac{m_f k_s}{2\sqrt{\pi}x_2} \left(\frac{1}{x_1} + \frac{1}{x_1 + x_2} \right) \psi_{hh'}(x_1 + x_2, x_3) \\ &- \frac{m_f k_s}{2\sqrt{\pi}x_2} \left(\frac{1}{x_3} + \frac{1}{x_2 + x_3} \right) \psi_{hh'}(x_1, x_2 + x_3) \\ &- \text{Sgn}(\lambda) \frac{(hi\delta_{|\lambda|1} + \delta_{|\lambda|2})m_f k_a}{2\sqrt{\pi}x_2} \left(\frac{1}{x_1} - \frac{1}{x_1 + x_2} \right) \psi_{-hh'}(x_1 + x_2, x_3) \\ &+ \text{Sgn}(\lambda) \frac{(h'i\delta_{|\lambda|1} + \delta_{|\lambda|2})m_f k_a}{2\sqrt{\pi}x_2} \left(\frac{1}{x_3} - \frac{1}{x_2 + x_3} \right) \psi_{h-h'}(x_1, x_2 + x_3) \ . \end{aligned} \quad (115)$$

⁸With no truncation of Fock space the scale could be generated by wee parton effects [63].

As stated earlier, for full generality one should also allow the kinetic masses m_f^2 to be Fock sector dependent. The conventions of ref.[64] have been adopted for the instantaneous gluon kernels

$$K(\psi_{hh'}(x_1, x_2)) = \frac{1}{2\pi} \int_0^1 dy \left\{ \frac{\psi_{hh'}(x_1, x_2) - \psi_{hh'}(y, 1-y)}{(y-x_1)^2} \right\}, \quad (116)$$

$$\begin{aligned} K(\psi_{h(\lambda)h'}(x_1, x_2, x_3)) &= \frac{1}{2\pi} \int_0^{x_2+x_3} dy \frac{(x_3 + 2x_2 - y)}{2(x_3 - y)^2 \sqrt{x_2(x_2 + x_3 - y)}} \left\{ \psi_{h(\lambda)h'}(x_1, x_2, x_3) \right. \\ &\quad \left. - \psi_{h(\lambda)h'}(x_1, x_2 + x_3 - y, y) \right\} \\ &\quad + \frac{1}{2\pi x_3} \left(\sqrt{1 + \frac{x_3}{x_2}} - 1 \right) \psi_{h(\lambda)h'}(x_1, x_2, x_3) \\ &\quad + \frac{1}{2\pi} \int_0^{x_1+x_2} dy \frac{(x_1 + 2x_2 - y)}{2(x_1 - y)^2 \sqrt{x_2(x_1 + x_2 - y)}} \left\{ \psi_{h(\lambda)h'}(x_1, x_2, x_3) \right. \\ &\quad \left. - \psi_{h(\lambda)h'}(y, x_1 + x_2 - y, x_3) \right\} \\ &\quad + \frac{1}{2\pi x_1} \left(\sqrt{1 + \frac{x_1}{x_2}} - 1 \right) \psi_{h(\lambda)h'}(x_1, x_2, x_3). \end{aligned} \quad (117)$$

These coupled integral equations have to be solved numerically. Note that iterating the link-field emission terms, i.e. those terms in Eqs. (114) and (115) that mix different Fock components, one obtains a (logarithmically) divergent self-energy correction. In order to cancel this divergence, a divergent counter-term has been added to the second line of Eq. (114). In numerical calculations this divergence has to be regularized. In Ref. [61] this divergence is automatically regularized since in DLCQ integrals are replaced by summations, which has a similar effect on small x divergences as introducing a lower bound on the x integration. In Refs. [58, 62] an alternative regulator has been used, where link-field emission and absorption vertices are multiplied by a factor x^ϵ , where x is the momentum of the link field and $0 < \epsilon$ is a small regularization parameter.

In Ref. [61], a DLCQ basis was used to cast these coupled integral equations into matrix form. However, for theories with fermions, no improvement techniques [30, 31] have been developed yet to accelerate the convergence in the DLCQ parameter K , which is very slow as a consequence. If basis functions are used instead, a convenient choice is

$$\psi(x_{f_1}, x_{f_2}, \dots; x_{b_1}, x_{b_2}, \dots) = x_{f_1}^\alpha x_{f_2}^\alpha \dots x_{b_1}^{(\alpha+\frac{1}{2})} x_{b_2}^{(\alpha+\frac{1}{2})} \dots P(x_{f_1}, x_{f_2}, \dots; x_{b_1}, x_{b_2}, \dots), \quad (118)$$

where x_{f_i} and x_{b_i} denote longitudinal momentum fractions of fermions and bosons respectively and P belongs to a complete set of polynomials. In this ansatz the exponent for bosons (link fields), $\alpha + \frac{1}{2}$, is chosen in order to cancel the factors of $\frac{1}{\sqrt{x_b}}$ that typically arise at vertices involving bosons. That way, all necessary integrals can be performed analytically with such an ansatz, using again Eq. (61).

In actual calculations using Eqn. (118), α was not taken from an equation analogous to Eq. (59) available in the two-particle truncation, because the naive end-point behaviour gets renormalized anyway, due to mass renormalization for example. In all but the lowest Fock component, the wavefunction is in fact finite as the fermion momentum approaches zero [64]. However, as long as one uses a complete

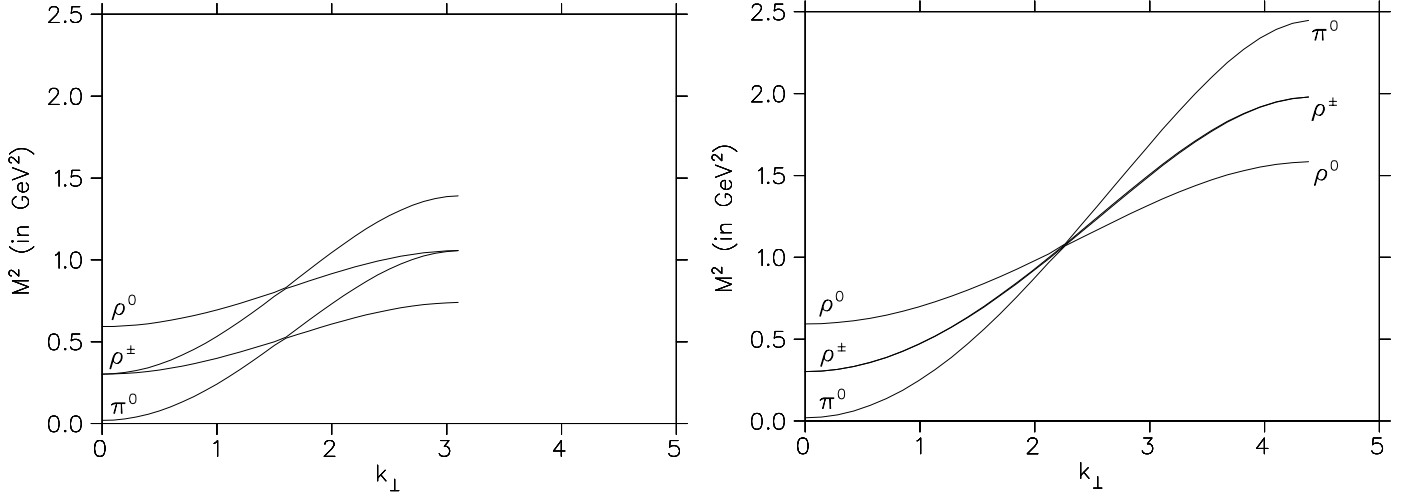


Figure 14: Dependence of $M^2 \equiv 2P^+P^-$ of π and ρ mesons on their transverse momentum k_\perp , for momenta along a lattice axis and along a diagonal respectively. The superscripts $\pm, 0$ refers to the helicity at $k_\perp = 0$. An exactly relativistic result should follow the form $M^2 = \mathcal{M}^2 + k_\perp^2$.

set of functions P in the expansion, the actual ansatz for the end-point behaviour does not matter in principle. It only matters from a practical point of view, since convergence in the Hilbert space expansion will be degraded by using a basis of functions with the wrong small momentum behaviour. The sensitivity to the x^ϵ regulator can be studied in final results, which should be finite in the limit that the regulator is removed (although convergence in the number of basis functions will be degraded as the regulator is made smaller). The basis function method was used to produce the results [62, 65] that we show later. After errors due to cut-off extrapolation have been quantified, these results are consistent with those obtained by DLCQ [61], indicating that both methods are giving reasonable results.

In the numerical calculations, $\alpha \in (0, 1)$ was picked and for a fixed value of α the convergence of physical observables as a function of the number of polynomials P was studied. For typical coupling choices that led to the correct meson masses and relativistic dispersion, this convergence was found to be sufficiently rapid for values of $\alpha \approx 0.5$. Typical results, which demonstrate the size of residual Lorentz symmetry breaking in the light mesons are displayed in Fig. 14. Future calculations including additional terms in P^- as well as higher Fock components can improve this situation.

Twist-2 distribution amplitudes for the helicity-zero π and ρ mesons are defined by (covariant normalisation)

$$\begin{aligned}
 f_\pi \phi_\pi(x) &= \int \frac{dx^-}{2\pi} \langle 0 | \bar{\Psi}(0) \gamma^+ \gamma_5 \Psi(x^-) | \psi_\pi(P) \rangle e^{ixP^+x^-} \\
 f_{\rho_0} \phi_{\rho_0}(x) &= \int \frac{dx^-}{2\pi} \langle 0 | \bar{\Psi}(0) \gamma^+ \Psi(x^-) | \psi_\rho(P) \rangle e^{ixP^+x^-} .
 \end{aligned}
 \tag{119}$$

Because of the appearance of the ‘good’ γ^+ components of the currents in Eq. (119), one can express these distributions entirely in terms of the two particle Fock component of these mesons

$$f_\pi \phi_\pi(x) = \frac{2}{a} \sqrt{\frac{N}{\pi}} \psi_{+-}^\pi(x)$$

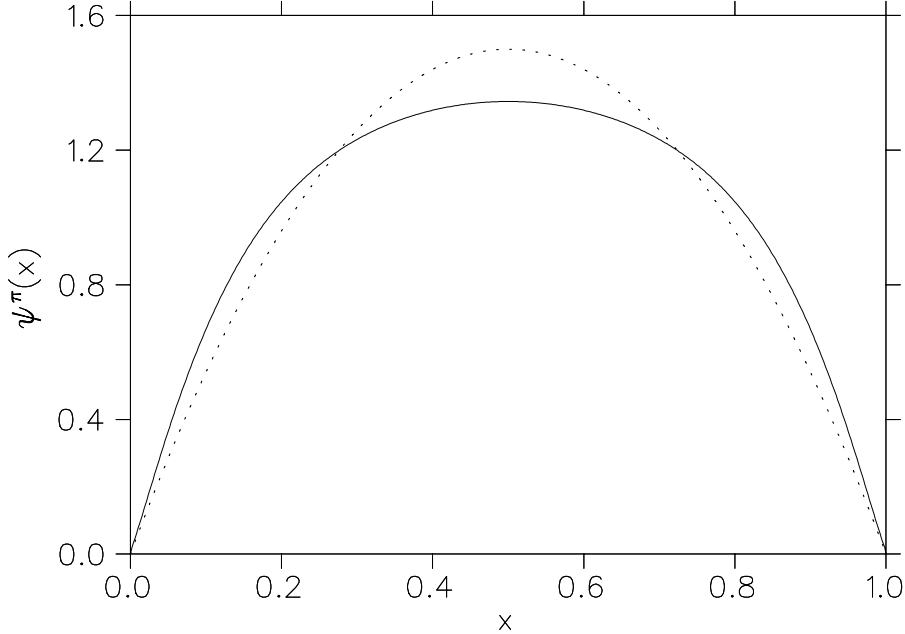


Figure 15: Pion distribution amplitude calculated on the transverse lattice. For comparison, the asymptotic shape is shown as a dashed line. Both curves are normalised to area one.

$$f_{\rho_0} \phi_{\rho_0}(x) = \frac{2}{a} \sqrt{\frac{N}{\pi}} \psi_{+-}^{\rho_0}(x) \quad (120)$$

where the distribution amplitudes are normalised to one; for example, $\int_0^1 dx \phi_\pi(x) = 1$.⁹

Using $N = 3$ in these formulae, the decay constants one calculates are $f_\pi \approx 300$ MeV and $f_{\rho_0} \approx 270$ MeV in the one-link approximation, which are larger than the experimental results of $f_\pi = 132$ MeV and $f_{\rho_0} = 216$ MeV [66]. This discrepancy is most likely caused by the Fock space truncation, since including higher Fock components tends to decrease the probability to find a hadron in its lowest Fock component and therefore also the normalization of the distribution amplitude. For the ρ meson the discrepancy is significantly smaller, suggesting perhaps that it is less sensitive to the chiral symmetry breaking aspects, that have only been crudely treated.

Results for the π distribution amplitude are shown in Fig. 15. Although $\phi_\pi(x)$ has some resemblance to the asymptotic distribution $\phi_{as}^\pi(x) = 6x(1-x)$ [67], the transverse lattice result is somewhat broader, but clearly does not exhibit any ‘double hump’ feature, found in early QCD sum rule analysis [5]. This distribution has recently been studied experimentally for the first time directly [68]. Conventional Euclidean lattice QCD simulations have yielded estimates of the second moment of $\phi_\pi(x)$ [69]. These results, together with the more recent ‘non-local’ QCD sum rule calculations [70], are all consistent with the single humped form. The ρ meson distribution amplitude from the transverse lattice looks similar, although it is slightly more peaked, which probably reflects the weaker binding of the quarks in the ρ .

In the light-cone framework, parton distributions are also very easy to evaluate, since they are momentum densities summed over all Fock components. For example, for the unpolarized distribution

⁹Note that the explicit expression given for f_π in Ref. [61] has an incorrect normalisation factor.

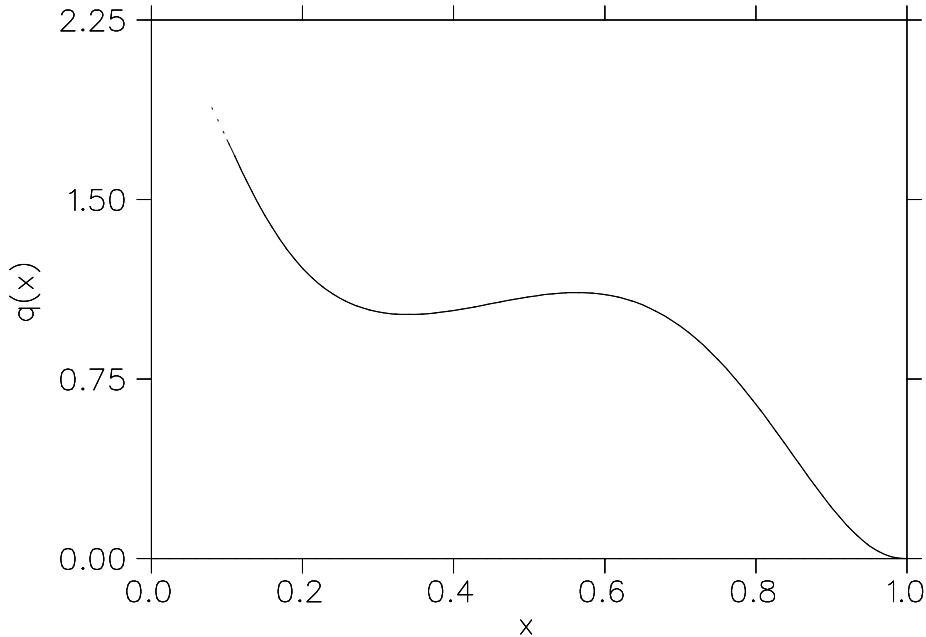


Figure 16: Quark distribution function Eq. (121) for the pion.

function for quarks one finds

$$q(x) = \sum_{h,h'} |\psi_{hh'}(x, 1-x)|^2 + \sum_{h,\lambda,h'} \int_0^{1-x} dy |\psi_{h(\lambda)h'}(x, y, 1-x-y)|^2 + \dots, \quad (121)$$

where \dots indicates contributions from higher Fock components that were not included in the present calculations. As an example, the distribution function from the transverse lattice for the π meson in the one-link approximation is shown in Fig. 16. The peak around $x \approx 0.5$ is mostly due to the $q\bar{q}$ Fock component, while contributions from higher Fock components dominate at smaller values of x . This distribution can be inferred from a fit to pion-nucleon Drell-Yan scattering [71], has been recently investigated in Dyson-Schwinger models [72], and has had the lowest moments measured in Euclidean lattice QCD [73]. More precise experimental data will soon be provided by the Jefferson laboratory, which will allow to compare more meaningfully the various theoretical predictions. Polarized parton distributions can be investigated in a similar manner, for mesons with spin [61].

Parton distribution functions are scale dependent. For the parton distribution functions calculated on the transverse lattice the relevant scale should be $Q_0 \sim \frac{1}{a}$, where $a \sim 0.5 - 0.7$ fm. Note that the precise relationship between this scale and those used in perturbative renormalisation schemes is unknown so long as one cannot match onto perturbation theory. Because of this uncertainty in scale setting and also because the use of perturbation theory at these low momentum scales is questionable, we do not show ‘evolved’ parton distribution functions here.

Another very interesting class of observables that are accessible on the transverse lattice are hadron form factors. For example, the pion elastic electromagnetic form factor defined by

$$\langle \psi(P') | j_{\text{em}}^\mu(q) | \psi(P) \rangle \equiv F(-q^2)(P' + P)^\mu. \quad (122)$$

In a light-cone framework, it is usually preferable to evaluate form factors in the Drell-Yan frame [74] ($q^+ = 0$, where q is momentum transfer). Only terms that are diagonal in Fock space (no pair creation terms) contribute to matrix elements of the ‘+’ component of current operators in this frame. From a practical point of view, this is a great advantage since one can then express the form factor entirely in terms of convolution integrals of Fock-space amplitudes for the initial and final state hadron. For space-like elastic form factors $F(-q^2)$, $q^2 = 2q^+q^- - \mathbf{q}^2 < 0$, it is always possible to choose a frame with $q^+ = 0$ and therefore $\mathbf{q}^2 = -q^2$. In terms of the 2 and 3 particle Fock space amplitudes on the transverse lattice one finds

$$\begin{aligned}
F(-q^2) &= \int_0^1 dx_1 dx_2 \sum_{h,h'} \delta(x_1 + x_2 - 1) |\psi_{hh'}(x_1, x_2)|^2 \\
&+ 2 \sum_{h,h',r} \int_0^1 dx_1 dx_2 dx_3 \delta(x_1 + x_2 + x_3 - 1) \cos\left(\left(x_1 + \frac{x_2}{2}\right) a \mathbf{q} \cdot \hat{\mathbf{r}}\right) |\psi_{h(r)h'}(x_1, x_2, x_3)|^2,
\end{aligned} \tag{123}$$

where we used the quadratic expression for the electromagnetic current $e\bar{\Psi}\gamma^\mu\Psi$ and used G-parity and transverse reflection symmetries to simplify the final expression. Note that the normalisation condition $F(0) = 1$ is ensured by the wavefunction normalisation Eq.(112)

The calculations in the one-link approximation yield a value for the root mean square radius of the pion, determined from $r_\pi^2 \equiv 6 \frac{d}{dq^2} (F(-q^2))_{q^2=0}$, of $r_\pi = (0.3 \pm .05 \text{ fm})$, where the main source of uncertainty is the transverse lattice spacing. This result is much smaller than the experimental value $r_\pi = 0.663 \text{ fm}$ [75]. Because we have truncated the Fock space above the three particle Fock component, the quark and antiquark cannot separate from each other by more than one lattice spacing, i.e. the quark or antiquark can separate from the center of mass¹⁰ only by about half the lattice spacing. This limit also represents a rough upper bound for the possible values of the rms radius and the numerical results come close to that limit. Another difficulty with evaluating form factors on the transverse lattice, using a large transverse momentum transfer, is that this will resolve the coarse lattice in the transverse direction.

We should emphasize that the restriction to the Drell Yan frame ($q^+ = 0$) is not absolutely necessary. One can evaluate meson form factors using purely longitudinal momentum transfers. Of course, since this necessarily implies $q^+ \neq 0$, one has to include matrix elements of the current operator that are off-diagonal in Fock space (change the number of partons). As long as no Fock space truncation is made, it is straightforward to include those off-diagonal terms. The off-diagonal contributions may be significant even if the probability to find additional $\bar{q}q$ pairs in the state is small as the following example illustrates: for N large, the amplitude to find two $\bar{q}q$ pairs in a meson meson scales like $\frac{1}{\sqrt{N}}$, i.e. the probability is $\frac{1}{N}$ suppressed. Nevertheless, since the vacuum to meson matrix element of the vector current operator scales like \sqrt{N} (while diagonal matrix elements are $\mathcal{O}(1)$), the off-diagonal terms still contribute to the same order in N as the diagonal terms and hence survive the large N limit. Therefore, even though higher $\bar{q}q$ Fock components are unimportant for the energy of the meson, they are still important in order to properly describe off-diagonal contributions to the form factor when $q^+ \neq 0$. This observation may also provide a clue as to how one could estimate these off-diagonal contributions to the form factor without explicitly enlarging the Fock space in the Hamiltonian, namely by calculating the mixing of the current with virtual meson states and then estimating the coupling of those virtual meson

¹⁰ Actually, it is the separation from the center of momentum that matters here, but for the qualitative discussion below this distinction is not very significant numerically.

states to the target hadron perturbatively. In fact, such a procedure has been successfully applied to derive and study exact expressions for off-diagonal contributions to form factors and generalised parton distributions in $QCD_{1+1}(N \rightarrow \infty)$ [76].

In summary, we have found that a wide range of observables have simple formulae in terms of the light-cone wavefunctions computed on the transverse lattice. Of course, the accuracy of the final results are then limited by the accuracy of the computed wavefunctions; the one-link approximation employed so far is not quantitatively realistic. Nevertheless, it is in principle straightforward to systematically relax this approximation. Alternatively, one could use larger quark masses, since mesons containing heavier quarks tend to be smaller and therefore may be affected less by a Fock space truncation. In addition, one would intuitively expect that a constituent picture works better for heavier quarks. Of course, for mesons containing both a heavy quark and a heavy antiquark one may run into the opposite problem, namely that large intrinsic transverse momenta start to resolve the very coarse transverse lattice. For quarks with masses on the order of strange quark masses this may not yet be a serious problem.

4.3 *B mesons on the transverse lattice*

In the limit where the b quark is infinitely heavy, it acts as a static colour source to which the light quark is bound. The structure of the light degrees of freedom becomes independent of the mass of the heavy source in this limit. Therefore, even though the dynamics of the light degrees of freedom in such a ‘heavy-light’ system is still as complex as in light mesons, a new symmetry (the heavy quark symmetry) emerges, which allow one to relate matrix elements from different heavy-light systems to one another. Symmetry to decays of B and D mesons play an important role in the determination of Standard Model parameters. Of course, even though the heavy quark symmetry allows to relate many hadronic matrix elements to one another, it still leaves many matrix elements as unknown parameters, which must be determined either by fit to experimental data or by nonperturbative QCD calculations.

A general method to introduce static sources into the light-cone formalism has been introduced in Ref. [78] and is very similar to the methods that were used in calculations of the static quark antiquark potential that were described in Section 3. However, the extension of the light meson calculations to such a heavy-light system can also be done by working with heavy quarks that have a finite mass and simply making that mass very large. Since the static source that the heavy quark represents does not propagate, no new parameters, such as hopping parameters, appear in the Hamiltonian for such a system. The latter was the approach chosen in Ref. [65], for a calculation in the one-link approximation that we now briefly review.

An important parameter in B meson phenomenology is the ‘binding energy’ $\bar{\Lambda} = m_B - m_b + \mathcal{O}\left(\frac{1}{m_b}\right)$. Different possibilities for its calculation exist. For example, one can directly use the numerically calculated energy eigenvalues, or one can extract $\bar{\Lambda}$ from the average light-cone momentum carried by the light degrees of freedom. In either case, the resulting value of $\bar{\Lambda} \approx 1.0$ GeV, found in ref.[65] in the one-link approximation, is larger than results obtained using other methods. For example, using Schwinger-Dyson techniques, one finds [79] $\bar{\Lambda} \approx 0.7$ GeV and Euclidean lattice gauge theory calculations yield [80] $M_B - M_b \approx 0.9$ GeV. It is not yet clear what causes $\bar{\Lambda}$ to be large in these transverse lattice calculations, but it is conceivable that higher Fock components will lead to a partial screening of the longitudinal string tension and hence a lowering of $\bar{\Lambda}$.

For the decay constant, which also plays an important role in B-meson phenomenology, $f_B \approx$

240 MeV \pm 20 MeV is found in the same approximation, also larger than those obtained using other methods. For example, Euclidean lattice gauge theory [81] and Dyson-Schwinger models [79] yield $f_B = 175$ MeV and $f_B = 182$ MeV respectively (it has yet to be accurately measured experimentally). However, the discrepancy is much smaller than for f_π . This result is consistent with the observation that the Fock expansion also seems to converge much more rapidly for B mesons. One should not be surprised to find more realistic results for B -mesons than for the π in the one-link approximation. On the basis of vector meson dominance, both hadrons are expected to have an rms radius of about $\frac{2}{3}$ fm. In the case of the B meson however, the rms radius is the average distance between the static source and the light quark, while the rms in the π is given by the average distance from the center of mass (or momentum), which is about half the separation between q and \bar{q} . Since the Fock space truncation did not allow for separations between q and \bar{q} of more than 0.7 fm in both calculations, the quark in the π could not separate from the center of mass by more than 0.35 fm while the q in the B -meson can separate from the center of mass by 0.7 fm. The more rapid convergence of the Fock expansion is also not unexpected. The static quark in the B meson does not ‘hop’ and therefore it is not dressed with virtual link quanta. Therefore, already if one neglects interference effects due to exchanged link quanta, one would expect about twice as many link quanta in light-light mesons as compared to heavy-light mesons, from dressing of quarks.

The B -meson (twist two) distribution amplitude, which plays an important role in exclusive B decays is shown in Fig. 17. In the limit $m_b \rightarrow \infty$, the b quark carries 100% of the momentum of the B -meson. For finite, but large m_b the wave function is localized near the region where the b quark carries momentum fraction $1 - \frac{\bar{\Lambda}}{m_b} < x_b < 1$. We therefore rescale the B meson distribution amplitude in such a way that it has a finite $m_b \rightarrow \infty$ limit

$$\phi_\infty(z) \equiv \lim_{m_b \rightarrow \infty} \frac{1}{\sqrt{m_b}} \psi_{m_b} \left(1 - \frac{z}{m_b} \right), \quad (124)$$

where $x_b = 1 - \frac{z}{m_b}$ is the momentum fraction carried by the b quark. The peak of $\phi_\infty(z)$ is localized at comparatively large momenta, which is consistent with the large value $\bar{\Lambda} \approx 1.0$ GeV that was found numerically from the ‘binding energy’ and from the momentum carried by the light degrees of freedom.

For phenomenological applications [82], it is most important to know the moments, where one finds

$$\begin{aligned} \frac{\int_0^\infty dz \phi_\infty(z) z}{\int_0^\infty dz \phi_\infty(z)} &\approx 1.22 \text{ GeV} \approx 1.2 \bar{\Lambda} \\ \frac{\int_0^\infty \frac{dz}{z} \phi_\infty(z)}{\int_0^\infty dz \phi_\infty(z)} &\approx 1.51 \text{ GeV}^{-1} \approx 1.5 \bar{\Lambda}^{-1}. \end{aligned} \quad (125)$$

Another important observable in B -physics is the Isgur-Wise (IW) form factor [83], because of its use for extracting the CKM matrix element V_{bc} from decays like $B \rightarrow \bar{D}^* l \nu$. We work in the limit $m_c, m_b \rightarrow \infty$, where matrix elements like $\langle B' | \bar{b} \gamma^\mu b | B \rangle$, $\langle D^* | \bar{c} \gamma^\mu b | B \rangle$ are all described by the same universal form factor

$$\langle B' | \bar{b} \gamma^\mu b | B \rangle = m_B (v'^\mu + v^\mu) F(v \cdot v'), \quad (126)$$

with v the velocity of the heavy quark. For $m_b, m_c \gg \Lambda_{QCD}$, heavy quark pair creation is suppressed, i.e. the relevant matrix element is diagonal in Fock space and an overlap representation exists for $F(v \cdot v')$ [65]

$$F(v \cdot v') = F^{(2)}(v \cdot v') + F^{(3)}(v \cdot v'), \quad (127)$$

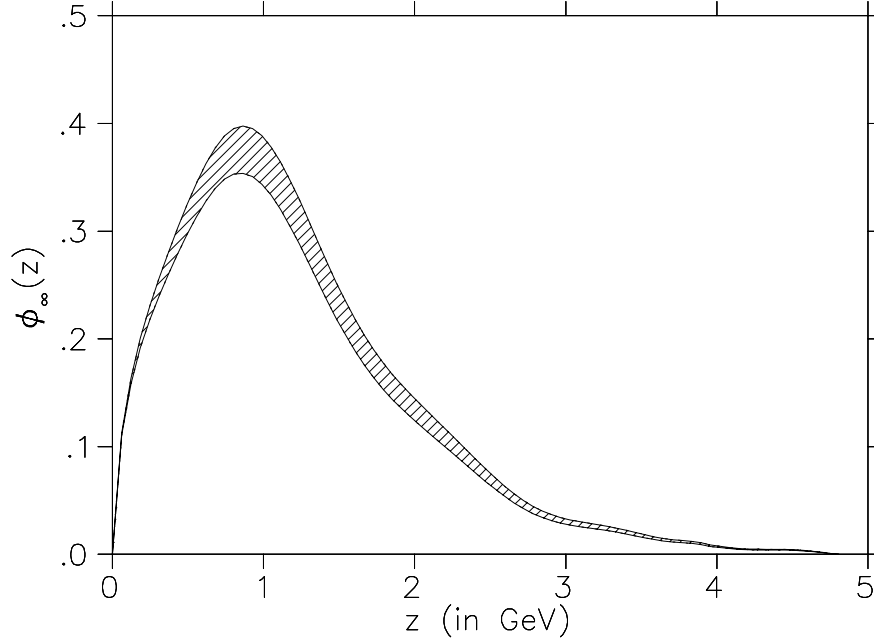


Figure 17: Heavy meson distribution amplitude Eq. (124) in the heavy quark limit. The shaded area reflects numerical uncertainties in the extrapolation $m_b \rightarrow \infty$.

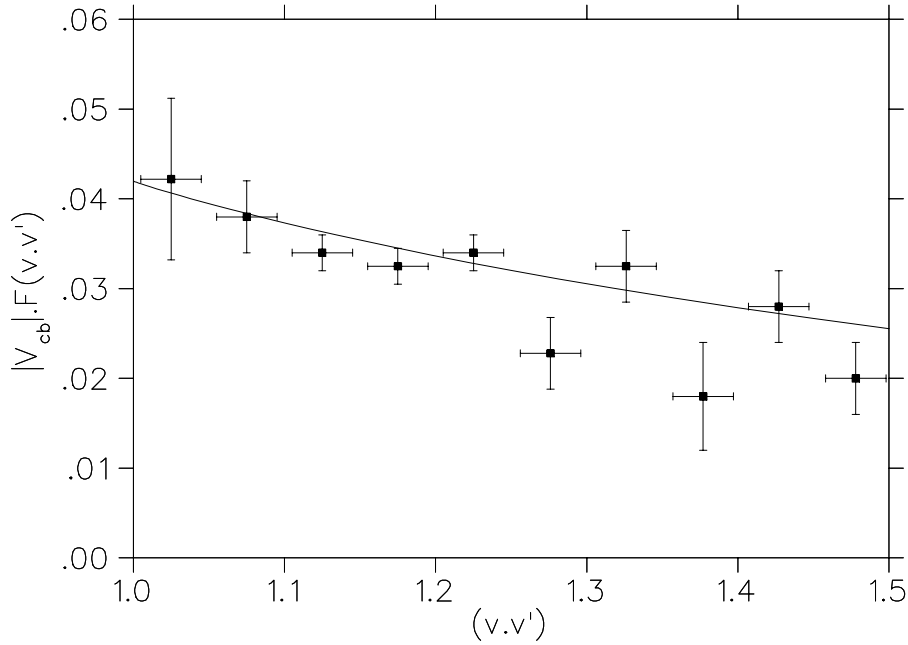


Figure 18: Isgur-Wise form factor Eq. (127) in the heavy quark limit. The experimental data is from Ref. [84].

where

$$\begin{aligned}
F^{(2)}(x) &= \frac{2}{2-x} \sum_s \int_x^1 dz \psi_s(z) \psi_s^* \left(\frac{z-x}{1-x} \right) \\
F^{(3)}(x) &= \frac{2}{2-x} \frac{1}{\sqrt{1-x}} \sum_s \int_x^1 dz \int_0^{1-z} dw \psi_s(z, w) \psi_s^* \left(\frac{z-x}{1-x}, \frac{w}{1-x} \right).
\end{aligned}
\tag{128}$$

If the heavy quarks were not infinitely heavy then pair creation terms, i.e. contributions where the current acts off-diagonally in Fock space, would contribute to form factors in addition to these overlap terms. In fact, the natural suppression of such terms in the limit where b quarks are static was one of the motivations for treating them as static sources in Ref. [65].

Results for the shape of the IW form factor, obtained from the numerically determined eigenstates on the transverse lattice, are shown in Fig. 18. The overall normalisation, which involves the CKM matrix element V_{bc} , was adjusted to agree with the data near zero recoil $v \cdot v' = 1$. As one can see in Fig. 18, the slope and shape of the nonperturbative transverse lattice results are consistent with experimental results. The functional form of the form factor obtained on the transverse lattice (which is also shown in Fig. (18) reads

$$F(v \cdot v') = 1 - 1.40(v \cdot v' - 1) + 1.72(v \cdot v' - 1)^2 - 0.20(v \cdot v' - 1)^3 - 1.82(v \cdot v' - 1)^4.
\tag{129}$$

Although theoretical constraints on the shape and slope of the form factor are very useful for extrapolating the experimental data to zero recoil, it would also be very useful to determine the $\frac{1}{m_b^2}$ corrections at zero recoil nonperturbatively, since those corrections represent a major source of uncertainty in extracting V_{cb} from the data. In order to estimate those corrections on the transverse lattice, it is first of all necessary to allow the heavy quarks to propagate. The most straightforward procedure would be to repeat the same method that was used to determine the hopping parameters for the light quarks. A less trivial complication will be the inclusion of those terms in the $b \rightarrow c$ current operator that are off-diagonal in the Fock space, i.e. which correspond to a virtual $\bar{b}c$ meson in the intermediate state.

5 Summary and Outlook

Light-cone variables allow a very physical approach towards a nonperturbative first principles description of many high-energy scattering observables, such as parton distributions measured in deep-inelastic scattering experiments. More generally, quantization of QCD on a null plane offers many advantages when tackling relativistic bound state problems. The transverse lattice is an extremely powerful framework to formulate and numerically solve QCD quantized in this way. Keeping the longitudinal x^\pm directions continuous preserves manifest boost invariance in one direction, while employing a spatial lattice regulator together with flux link-fields in the transverse direction maintains some gauge invariance. The transverse lattice thus combines advantages of lattice gauge theories with those of light-cone quantization. In the colour-dielectric formulation of transverse lattice QCD, linearized link field variables facilitate the formulation of an approximation scheme for the light-cone Hamiltonian which realises a constituent approach to hadrons. In this work, we have reviewed results from studies of glueballs and mesons within such a framework.

For the effective link-field interactions in pure gauge theory, a colour-dielectric expansion was made that included all terms up to fourth order that are consistent with the symmetries that are not broken by

the transverse lattice. In the large N limit this theory dimensionally reduced to 1+1 dimensions, greatly simplifying the calculation. The coefficients (‘coupling constants’) in this expansion were determined by seeking regions of enhanced Lorentz symmetry in coupling constant space. That way, the light-cone Hamiltonian for pure glue can be accurately determined from first principles, using only the string tension as input to fix the overall scale. Empirically, a one-dimensional subspace in coupling constant space — the renormalised trajectory — is found along which Lorentz symmetry is greatly enhanced and physical observables are nearly constant. Along this trajectory, observables are evaluated and numerical results for $N \rightarrow \infty$ glueball spectra obtained on the transverse lattice agree with extrapolations of finite N Euclidean lattice gauge theory calculations. These results not only provide strong evidence for the validity of the $\frac{1}{N}$ expansion of glueball masses, but at the same time provide an important consistency test for the colour-dielectric formulation of gauge theories on a transverse lattice. The corresponding light-cone wavefunctions suggest much more complex glueball structure than naive extrapolation of constituent gluon ideas would indicate, even at resolution scales of order 1 GeV.

Calculations with fermions have so far only been performed in a truncated Fock space basis, where no more than one link quantum was allowed. Since this implies that the transverse separation between q and \bar{q} in a meson can never exceed one lattice spacing, i.e. 0.5 – 0.7 fm in the present calculations, this is clearly too little separation between q and \bar{q} to accommodate even the smallest mesons, with an rms radius of about 0.7 fm. Therefore, it is not very surprising that the numerical results for mesons exhibited a larger violation of Lorentz symmetry than in the studies of glueballs.

In the glueball calculations on the transverse lattice the only input parameter was the confinement scale. Ideally, an extension of these calculations to mesons should have used only quark masses as additional parameters. However, because of the severe approximation of the Fock space involved and because the leading approximation of the Hamiltonian does not obviously incorporate spontaneous chiral symmetry breaking effects properly, one phenomenological input parameter (a chiral symmetry breaking scale) had to be used in order to obtain reasonable solutions.

Despite these drawbacks, qualitatively interesting results for the structure of mesons were obtained in the one-link approximation. For example, the pion distribution amplitude was found to be single humped and its shape was not far from the asymptotic shape, although the normalisation, set by f_π , is much larger than the experimental value. About 25% of the momentum of π and ρ mesons is carried by gluonic degrees of freedom (the link fields) at the transverse resolution scale of order 1 GeV. This is somewhat smaller than experiment. The quantitative discrepancies are all consistent with the fact that, because of probability conservation, the one-link approximation overestimates the pure $\bar{q}q$ contribution to Fock space. About half the ρ meson helicity is found to be carried by quark and antiquark helicity [61]. The rest resides in orbital angular momentum and gluon spin.

Including a static heavy quark into the above formalism is straightforward and requires no additional parameters in the Hamiltonian. The parameters in the effective Hamiltonian can be taken from the light meson and glueball calculations. Both $\bar{\Lambda}$, the binding energy of B-mesons, and the decay constant f_B come out relatively large compared to other calculations and phenomenological models, although the discrepancy is less than what it is for f_π . Excellent agreement between the calculated slope of the Isgur-Wise form factor and experimental data from $B \rightarrow D^*$ decays is obtained.

For many phenomenological applications, it will be necessary to extend the analysis to baryons; at the time of writing, no comprehensive work has yet been performed on the transverse lattice, although in principle it is straightforward. Since this will be a very important direction for the future, let us briefly indicate the new features that will arise. In the studies of mesons presented in Section 4, we

formally made use of a large N approximation when classifying operators, in order to be consistent with the pure-gluon studies. However, in a Fock space truncated to $q\bar{q}$ and $qM\bar{q}$, numerical results are independent of N . For example, non-planar diagrams which would involve crossing of link fields would require at least two intermediate link fields. For baryons, of course, the value of N is determined by the number of quarks in the valence component. For finite N , there is an additional class of operators, compatible with the (gauge) symmetries on the transverse lattice, that one should consider; namely, operators involving the determinant of the link fields. For $N = 3$, such a term $\propto \text{Re det}[M]$ is cubic in the fields and, since we have otherwise included all possible terms up to 4^{th} order, we should include such a term in the renormalised Hamiltonian

$$P_{det}^- \equiv \sum_{\mathbf{x}} \int dx^- \mathcal{H}_{det}(M) = \sum_{\mathbf{x}} \int dx^- \sum_r \det[M_r] + \det[M_r^\dagger]. \quad (130)$$

All other additional operators that one can include are of higher order. The richer Fock space structure, as well as the additional mixing of Fock sectors induced by the determinant interaction Eq. (130), requires previous ($N = \infty$) calculations to be repeated in order to redetermine the coefficients of all terms in the renormalised Hamiltonian. One of the most important roles played by \mathcal{H}_{det} is in the lattice propagation of baryons, which is also crucial for the spin splitting between the nucleon and the Δ .

Compared to many other techniques, the transverse lattice is still largely uninvestigated. The next applications in hadronic physics will require the extension of Fock space truncation beyond one link to allow lighter mesons to expand nearer their physical size, the study of baryons, finite quark mass corrections in B meson studies, and eventually the inclusion of $\bar{q}q$ pair production effects. At the formal level, it will be interesting to see if symmetry (including parity [85]) is enough to fix all parameters in the quark sector and beyond the leading order of the colour-dielectric expansion. In the quark sector, this ultimately entails a first principles understanding of how spontaneous chiral symmetry breaking manifests itself in the renormalised Hamiltonian. Even if symmetry is not enough, perhaps only a discrete phenomenological input needs to be introduced to determine all couplings accurately. The predictive power is still enormous, since entire functions of momentum are determined. Although a typical coarse transverse lattice Hamiltonian contains many parameters, (almost) all of them are determined by symmetry alone.

Acknowledgments M.B. was supported by the Department of Energy (DE-FG03-96ER40965) and by Deutsche Forschungsgemeinschaft and would like to thank W.Weise and the nuclear theory group at TU München for their hospitality while finishing this manuscript. S.D. was supported by the Particle Physics and Astronomy Research Council grant no. GR/LO3965.

A Miscellaneous Remarks about Fermions

There are a number of subtle issues related to fermions within the light-cone framework that need to be addressed also by transverse lattice calculations. These are issues that arise because of small k^+ divergences caused by the particular momentum dependence of the coupling of fermions to link-fields. Of course, small k^+ divergences also arise in the pure gluon formulation of the transverse lattice. However, in that case it seems that adding the appropriate one loop mass counterterms (often called self-induced inertias within the light-cone framework) takes care of these problems. Furthermore, if one maintains gauge invariance many divergences at small k^+ cancel among each other. When fermions are included,

new small k^+ divergences arise from Yukawa-type couplings to the transverse gauge field degrees of freedom. Below we discuss the two most important complications and ways to deal with them.

A.1 Momentum dependent mass counterterms

The coupling of quarks to link fields on the transverse lattice has a longitudinal momentum dependence that is similar to the one for Yukawa theories, e.g.

$$\mathcal{H}^{(3)} \propto i\kappa \left(\frac{1}{k_{in}^+} - \frac{1}{k_{out}^+} \right) \frac{1}{\sqrt{k_b^+}}, \quad (131)$$

where k_{in}^+ and k_{out}^+ are initial and final fermion momenta, and k_b^+ the boson momentum. In second order perturbation theory, this type of interaction leads to logarithmically divergent self-energies for the fermion. For a fermion of momentum p^+ the shift in light-cone energy is

$$\Delta^{(2)}P^- \sim \kappa^2 \int_0^{p^+} \frac{\left(\frac{1}{k^+} - \frac{1}{p^+}\right)^2}{P^- - \frac{m^2}{2k^+} - \frac{m_g^2}{2(p^+ - k^+)}} dk^+ . \quad (132)$$

Because of this divergence, a regulator for small longitudinal momenta needs to be introduced and counterterms need to be added to compensate the divergence.

The issues that arise in this context are the Fock sector and momentum dependence of mass counterterms. The Fock sector dependence is easy to understand. For example, if one truncates the Fock space above states with one boson (link quantum) ‘in flight’, then the above mass renormalization only affects quark masses in the sector without the boson, since only in that sector would the allowed Fock space permit adding another boson. Therefore, within the colour dielectric expansion one needs to treat the masses of the quarks in different Fock sectors as independent parameters. Of course, ultimately they are not independent, but the relation between the masses in different Fock sectors is dynamical and nonperturbative.

A more subtle issue is the momentum dependence of mass counterterms. If one employs a regularization scheme that breaks the manifest boost invariance in the longitudinal direction, then one should not expect momentum independent mass counterterms either. A popular example for such a regularization scheme is DLCQ [29], where (anti-) periodicity conditions in the x^- direction lead to momenta that are integer (or half integer) multiple of some momentum unit. In such a scheme the self mass $P^+\Delta^{(2)}P^-$ depends on P^+ because the phase space that is allowed for the intermediate states does depend on the value of integer momentum of the quark. In order to properly compensate for this fact, it is in general necessary to introduce a momentum dependent mass counterterm in DLCQ.¹¹ Transverse lattice calculations with fermions that have been performed so far (using DLCQ as well as continuum basis functions) included a maximum of one link quantum in flight. As a result the momentum dependence of the self-energy is easily calculable and the divergent part is cancelled by adding the so-called self-induced inertia terms [29]. However, future calculations which include more Fock components will have to deal with this issue. A couple of options might be practical:

¹¹Although contemporary DLCQ calculations usually include the momentum dependent $\mathcal{O}(\kappa^2)$ mass counterterm, higher order momentum dependent counterterms have usually not been treated in this framework.

- Using regulators that maintain manifest boost invariance in the longitudinal direction. For example, if one expands states using complete sets of continuous basis functions, one ends up with matrix elements in the Hamiltonian that involve overlap integrals of basis functions and operators. Those integrals can be regulated in a boost invariant manner, for example by introducing cutoffs on ratios of momenta. The integrand is multiplied by a factor $\left(k_{after}^+/k_{before}^+\right)^\varepsilon$, where $k_{before/after}^+$ is the quark momentum before/after emitting a link quantum and ε is some small number. Calculations are performed at finite ε and observables are extrapolated to $\varepsilon \rightarrow 0$ at the end of the calculation.
- One of the reasons for the popularity of DLCQ is that it is relatively easy to develop computer code for non-perturbative calculations. This advantage also applies to transverse lattice calculations and it is therefore worthwhile to investigate if one can modify DLCQ in such a way that one can cope with the momentum dependent counterterms. In more ambitious studies that include higher Fock components one may imagine allowing the bare mass (the term in the Hamiltonian) to depend on the integer momentum and to fix this momentum dependence of this bare mass nonperturbatively by some means. For example, one could demand that hadron masses are approximately independent of the total (integer) momentum of the hadron.

A.2 Vertex mass renormalisation

In the common light-cone quantization procedure for field theories involving fermions one normally uses the constraint equation to eliminate the non-dynamical spinor components $\Psi_{(-)}$. Even if the original Lagrangian involves only couplings of fermions to bosons that are linear in the boson field, the effective Lagrangian for the dynamical component $\Psi_{(+)}$ usually also involves terms where the fermions couple to the second power of the boson field (Fig. 19a). In Ref. [86], it was shown that this four-point interaction can lead to large non-perturbative corrections of the three point coupling of the fermions to bosons. Loop corrections, such as the ones depicted in Fig. 19 b and c, may effectively enhance the three-point couplings. This may have important effects. For example, the higher order corrections to the tree level three point interaction Eqn. (131) lead to an effective enhancement $\kappa \rightarrow \kappa_{ren}$, where κ_{ren} can differ significantly from κ . These fundamental observations have several important practical consequences.

A.2.1 Three point vertex in the chiral limit

In the chiral limit of QCD, helicity is conserved in perturbation theory. This reflects itself in the fact that the three point quark helicity flip vertex in the canonical light-cone Hamiltonian for QCD is linear in the quark mass. If one would simply set this term to zero in the chiral limit, the dynamics would become completely independent on the quark helicity — yielding π 's that are degenerate with ρ 's and nucleons that are degenerate with Δ 's. The resolution to this apparent paradox lies in the abovementioned observation that non-perturbative effects (from very high Fock components) can give rise to an enhancement of κ such that the helicity-flip vertex amplitude for dressed quarks may not vanish — even if it does so at any finite order in perturbation theory.

In a truncated Fock space, such nonperturbative enhancements would be suppressed and it is thus necessary to allow the three-point coupling to remain finite in the chiral limit in order to mimic this enhancement which would be present without Fock space truncation. This observation explains why it

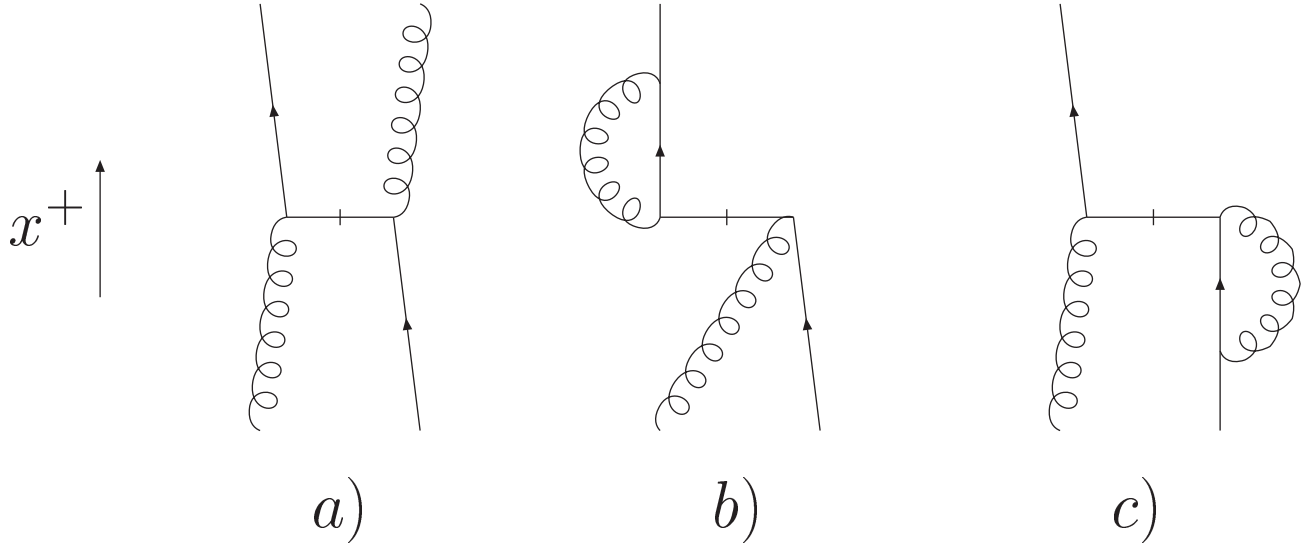


Figure 19: a) interaction for the dynamical fermion component that is induced by eliminating the constrained component of the fermions $\Psi_{(-)}$. The slashed horizontal (x^+ instantaneous) fermion line represents the eliminated degrees of freedom. b) higher order correction to the three point function (boson absorption), which involves this four point coupling. c) same as b), but with a different time ordering of the interactions.

is fallacious in calculations with Fock space truncation to argue that the chiral limit corresponds to the subspace in parameter space where the quark helicity flip coupling for the quarks vanishes.

A.2.2 Fock sector dependent vertex renormalisation

Imposing a cutoff on the Fock space also leads to an asymmetric treatment of loop corrections to the vertex in the initial and final state. For example, consider the process of boson absorption by a quark (Fig. 19 b,c). If the Fock space truncation is such that only one boson is allowed ‘in flight’, then vertex corrections in the initial state (Fig. 19 c) are suppressed. The practical consequence of such an asymmetric renormalisation is that one generates an effective three-point coupling that involves fermion momenta in an asymmetric way [86, 58]

$$\mathcal{H}^{(3)} \propto i\kappa \left(\frac{1}{k_{in}^+} - \frac{1}{k_{out}^+} \right) \frac{1}{\sqrt{k_b^+}} \longrightarrow i \left(\frac{\kappa}{k_{in}^+} - \frac{\kappa_{ren}}{k_{out}^+} \right) \frac{1}{\sqrt{k_b^+}} . \quad (133)$$

Since, as we emphasized above, the enhancement κ_{ren} vs. κ can be significant, one would in principle have to introduce Fock sector dependent three point couplings, for example

$$\mathcal{H}^{(3)} \rightarrow i \left(\frac{\kappa_{in}}{k_{in}^+} - \frac{\kappa_{out}}{k_{out}^+} \right) \frac{1}{\sqrt{k_b^+}} , \quad (134)$$

where ‘in’ and ‘out’ are defined in reference to the absorbed boson, and treat them as independent parameters.

In addition to this proliferation of three-point couplings, that is necessary once four-point interactions of Fig. 19 are included, there are many other types of four-point interaction between quarks and link fields allowed. Therefore, before enlarging the space of couplings one should have some physical criterion for selecting these four-point couplings. In all transverse lattice calculations to date, only the four-point interaction mediated by the instantaneous gluons A_+ has been included, since this is responsible for confinement.

Given the complications that are introduced by cutting off the Fock space, it becomes clear that one should ultimately avoid such truncations. Of course, strictly speaking it is impossible to work without any Fock space restrictions. However, with appropriate cutoffs on energy (or invariant mass) differences at each vertex, one may succeed to achieve that truncating very high energy Fock components has only a negligible impact on the low energy dynamics. If there is a cutoff ΔE on ‘allowed’ energy (or invariant mass) differences at a vertex, then very high energy states that have an energy that is several ΔE higher than the ground state are connected to the ground state only by several orders of the interaction. Therefore, cutting off such high energy states should have only little effect on low energy dynamics and one should thus be able to ignore problems that may in principle arise due to Fock space truncation.

References

- [1] W. A. Bardeen and R. B. Pearson, *Phys. Rev. D* 14 (1976) 547
- [2] S. Brodsky, G. McCartor, H-C. Pauli, and S. S. Pinsky, *Particle World* 3 (1993) 109
S. Brodsky, H-C. Pauli, and S. S. Pinsky, *Phys. Rep.* 301 (1998) 299
- [3] M. Burkardt, *Adv. Nucl. Phys.* 23 (1996) 1
- [4] I. Montvay and G. Munster, *Quantum Fields on a Lattice* (Cambridge University Press, 1994)
- [5] V. L. Chernyak and A. R. Zhitnitsky, *Phys. Rep.* 112 (1984) 173
- [6] E. V. Shuryak, *Phys. Rep.* 264 (1996) 357
E. V. Shuryak and T. Schafer, *Ann. Rev. Nucl. Part. Sci* 47 (1997) 359
- [7] C. D. Roberts and S. M. Schmidt, *Prog. Part. Nucl. Phys.* 45S1 (2000) 1
- [8] L. Susskind, *Phys. Rev.* 165 (1968) 1535
- [9] J. B. Kogut and D. E. Soper, *Phys. Rev. D* 1 (1970) 2901
- [10] K. G. Wilson, *Phys. Rev. D* 10 (1974) 2445
- [11] J. B. Kogut and L. Susskind, *Phys. Rev. D* 11 (1975) 395
- [12] P. A. Griffin, *Nucl. Phys. B* 139 (1992) 270
- [13] J. Wess and B. Zumino, *Phys. Lett. B* 37 (1971) 95
- [14] E. Witten, *Commun. Math. Phys.* 92 (1984) 455
- [15] P. A. Griffin, in Proceedings *Polana Light Cone Quantization* pp0240-245 (1994), Ed. S. Glazek, hep-th/9410243
- [16] H.-J. Pirner, *Prog. Part. Nucl. Phys.* 29 (1992) 33
- [17] D. Weingarten, *Phys. Lett. B* 90 (1980) 280
- [18] G. Mack, *Nucl. Phys. B* 235 (1984) 197

- [19] J. B. Kogut and L. Susskind, *Phys. Rev. D* 9 (1974) 3501
- [20] G. 't Hooft, *Nucl. Phys. B* 75 (1974) 461
- [21] S. S. Shei and H. S. Tsao, *Nucl. Phys. B* 141 (1978) 445
- [22] W. A. Bardeen, R. B. Pearson, and E. Rabinovici, *Phys. Rev. D* 21 (1980) 1037
- [23] T. N. Tomaras, *Nucl. Phys. B* 163 (1980) 79
- [24] K. Hornbostel, Ph. D Thesis, SLAC-PUB No. 333 (1988)
- [25] S. Dalley, *Phys. Rev. D* 58 (1998) 087705
- [26] A. Casher, *Phys. Rev. D* 14 (1976) 452
T. Maskawa and K. Yamawaki, *Prog. Theor. Phys.* 56 (1976) 270
C. Thorn, *Phys. Lett. B* 70 (1977) 77
- [27] V. A. Franke, Yu. A. Novozhilov, and E. V. Prokhvatilov, *Lett. Math. Phys.* 5 (1981) 239
F. Lenz, M. Thies, S. Levit, and K. Yazaki, *Ann. Phys. (N.Y.)* 208 (1991) 1
F. Lenz, H. W. L. Naus, M. Thies, *Ann. Phys. (N.Y.)* 233 (1994) 317
H-C. Pauli, A. C. Kalloniatis, and S. Pinsky, *Phys. Rev. D* 52 (1995) 1176
- [28] A. S. Mueller, A. C. Kalloniatis, H-C. Pauli, *Phys. Lett. B* 435 (1998) 189
- [29] H.-C. Pauli and S. J. Brodsky, *Phys. Rev. D* 32 (1985) 1993
- [30] S. Dalley and B. van de Sande, *Phys. Rev. D* 56 (1997) 7917
- [31] S. Dalley and B. van de Sande, *Phys. Rev. D* 59 (1999) 065008
- [32] M. Burkardt and B. Klindworth, *Phys. Rev. D* 55 (1997) 1001
- [33] G. 't Hooft, *Nucl. Phys. B* 72 (1974) 461
- [34] C. B. Thorn, *Phys. Rev. D* 20 (1979) 1435
- [35] T. Eguchi and H. Kawai, *Phys. Rev. Lett.* 48 (1983) 1063
S. R. Das, *Rev. Mod. Phys.* 59 (1987) 235
- [36] S. Dalley and T. R. Morris, *Int. J. Mod. Phys. A* 5 (1990) 3929
- [37] S. Dalley and I. R. Klebanov, *Phys. Rev. D* 47 (1993) 2517
- [38] G. Bhanot, U. M. Heller, and H. Neuberger, *Phys. Lett. B* 113 (1982) 47
- [39] S. Dalley and B. van de Sande, *Phys. Rev. Lett.* 82 (1999) 1088
- [40] S. Dalley and B. van de Sande, *Phys. Rev. D* 62 (2000) 014507
- [41] K. G. Wilson, *Phys. Rev. B* 140 (1965) 445
- [42] St. D. Glazek and K. G. Wilson, *Phys. Rev. D* 48 (1993) 5863
K. G. Wilson *et al.*, *Phys. Rev. D* 49 (1994) 6720
- [43] B. Lucini and M. Teper, *JHEP* 050 (2001) 0106
- [44] B. H. Allen and R. J. Perry, *Phys. Rev. D* 62 (2000) 025005
- [45] C. Csaki, H. Ooguri, Y. Oz, and J. Terning, *JHEP* 9901 (1999) 017
R. de Mello Koch, A. Jevicki, M. Mihailescu, and J. P. Nunes, *Phys. Rev. D* 58 (1998) 105009
C. Csaki, Y. Oz, J. Russo, and J. Terning, *Phys. Rev. D* D59 (1999) 065012 .
- [46] S. Dalley and B. van de Sande, *Phys. Rev. D* 63 (2001) 076004
- [47] M. Teper, *Phys. Rev. D* 59 (1999) 014512

- [48] C. Morningstar and M. Peardon, *Phys. Rev. D* 60 (1999) 0345509
- [49] Y. Nambu, *Phys. Rev. D* 10 (1974) 4262
- [50] L. Susskind, *Phys. Rev. D* 1 (1970) 1182
- [51] H. B. Nielsen and P. Olesen, *Nucl. Phys. B* 57 (1973) 367
- [52] N. Isgur and J. Paton, *Phys. Rev. D* 31 (1985) 2910
- [53] R. Hagedorn, *Nuovo Cimento Suppl.* 3 (1965) 147
- [54] H. Fritzsch and P. Minkowski, *Nuovo Cimento A* 30 (1975) 393
- [55] F. E. Close, G. R. Farrar, and Z-P. Li, *Phys. Rev. D* 55 (1997) 5749
- [56] H.B. Nielsen and M. Ninomiya, *Nucl. Phys. B* 185 (1981) 20 ; Erratum-ibid. *Nucl. Phys. B* 195 (1982) 541
- [57] P.A. Griffin, *Phys. Rev. D* 47 (1993) 3530
- [58] M. Burkardt and H. El-Khozondar, *Phys. Rev. D* 60 (1999) 054504
- [59] M. Burkardt, *Phys. Rev. D* 57 (1998) 1136
- [60] F. Lenz, M. Thies, and K. Yazaki, *Phys. Rev. D* 63 (2001) 045018
M. Burkardt, F. Lenz, M. Thies, and K. Yazaki, *to be published*
- [61] S. Dalley, *Phys. Rev. D* 64 (2001) 036006
- [62] M. Burkardt and S. Seal, invited talk at ‘Particle Physics Phenomenology 2000’, Taitung, Taiwan, Nov. 2000, hep-ph/0101338; *Phys. Rev. D* 65 (2002) 034501
- [63] A. Casher and L. Susskind, *Phys. Rev. D* 9 (1974) 436 .
- [64] F. Antonuccio and S. Dalley, *Phys. Lett. B* 376 (1996) 154
- [65] M. Burkardt and S. Seal, *Phys. Rev. D* 64 (2001) 111501(R)
- [66] D. E. Groom *et. al.*, *Eur. Phys. J. C* 15 (2000) 1
- [67] S. J. Brodsky and G. P. Lepage, in *Perturbative Quantum Chromodynamics*, ed. A. H. Mueller, (World Scientific Singapore, 1989)
- [68] E791 Collaboration, E. M. Aitala *et. al.*, *Phys. Rev. Lett.* 86 (2001) 4768
- [69] G. Martinelli and C. Sachrajda, *Phys. Lett. B* 190 (1987) 51 ; *Nucl. Phys. B* 306 (1988) 865
T. DeGrand and R. D. Loft, *Phys. Rev. D* 38 (1988) 954
T. Daniel, R. Gupta, and D. Richards, *Phys. Rev. D* 43 (1991) 3715
L. Del Debbio *et. al.*, *Nucl. Phys. B(Proc. Suppl.)* 83 (2000) 235
- [70] S. V. Mikhailov and A. V. Radyushkin, *Phys. Rev. D* 45 (1992) 1754
A. P. Bakulev and S. V. Mikhailov, *Phys. Lett. B* 436 (1998) 351
V. M. Braun, A. Khodjamirian, and M. Maul, *Phys. Rev. D* 61 (2000) 073004
- [71] M. Glück, E. Reya, and A. Vogt, *Z. Phys. C* 53 (1992) 651
- [72] M. B. Hecht, C. D. Roberts, and S. M. Schmidt, *Phys. Rev. C* 63 (2001) 025213
- [73] G. Martinelli and C. T. Sachrajda, *Phys. Lett. B* 196 (1987) 184
C. Best *et. al.*, *Phys. Rev. D* 56 (1997) 2743
- [74] S. D. Drell and T. M. Yan, *Phys. Rev. Lett.* 24 (1970) 181
- [75] S. R. Amendolia *et. al.*, *Nucl. Phys. B* 277 (1986) 168 .

- [76] M.B. Einhorn, *Phys. Rev. D* 14 (1976) 3451
M. Burkardt, *Phys. Rev. D* 62 (2000) 094003
- [77] M. B. Wise, in proceedings *Lepton Photon 2001*, Rome, July 2001, hep-ph/0111167
- [78] M. Burkardt, in Proceedings *Polana Light Cone Quantization*, pp 233-239 (1994), Ed. S. Glazek, hep-ph/9410219
- [79] M.A. Ivanov, Yu.L. Kalinovsky, and C.D. Roberts, proceedings for *Heavy Quark Physics 5*, Dubna, Russia, April 2000, hep-ph/0006189
- [80] S. Ryan, preprint hep-lat/0111010
- [81] C.T. Sachrajda, in proceedings *Lepton Photon 2001*, Rome, July 2001, hep-ph/01110304
- [82] M. Beneke and Th. Feldmann, *Nucl. Phys. B* 592 (2001) 3
- [83] N. Isgur and M. B. Wise, *Phys. Lett. B* 232 (1989) 113
- [84] CLEO collaboration, preprint hep-exp/0007052
- [85] M. Burkardt, *Phys. Rev. D* 54 (1996) 2913
- [86] M. Burkardt, *Phys. Rev. D* 58 (1998) 096015